

## Complete Nucleotide Sequence and Organization of the Atrazine Catabolic Plasmid pADP-1 from *Pseudomonas* sp. Strain ADP

Betsy Martinez, Jeffrey Tomkins, Lawrence P. Wackett, Rod  
Wing and Michael J. Sadowsky  
*J. Bacteriol.* 2001, 183(19):5684. DOI:  
10.1128/JB.183.19.5684-5697.2001.

---

Updated information and services can be found at:  
<http://jb.asm.org/content/183/19/5684>

---

### REFERENCES

*These include:*

This article cites 61 articles, 38 of which can be accessed free  
at: <http://jb.asm.org/content/183/19/5684#ref-list-1>

### CONTENT ALERTS

Receive: RSS Feeds, eTOCs, free email alerts (when new  
articles cite this article), [more»](#)

---

Information about commercial reprint orders: <http://jb.asm.org/site/misc/reprints.xhtml>  
To subscribe to to another ASM Journal go to: <http://journals.asm.org/site/subscriptions/>

## Complete Nucleotide Sequence and Organization of the Atrazine Catabolic Plasmid pADP-1 from *Pseudomonas* sp. Strain ADP

BETSY MARTINEZ,<sup>1</sup> JEFFREY TOMKINS,<sup>2</sup> LAWRENCE P. WACKETT,<sup>1,3,4</sup>  
ROD WING,<sup>2</sup> AND MICHAEL J. SADOWSKY<sup>3,4,5\*</sup>

*Department of Biochemistry, Molecular Biology and Biophysics,<sup>1</sup> Biological Process Technology Institute,<sup>3</sup> Center for Microbial and Plant Genomics,<sup>4</sup> and Department of Soil, Water & Climate,<sup>5</sup> University of Minnesota, St. Paul, Minnesota 55108, and Clemson University Genomics Institute, Clemson, South Carolina 29634<sup>2</sup>*

Received 25 January 2001/Accepted 2 July 2001

The complete 108,845-nucleotide sequence of catabolic plasmid pADP-1 from *Pseudomonas* sp. strain ADP was determined. Plasmid pADP-1 was previously shown to encode AtzA, AtzB, and AtzC, which catalyze the sequential hydrolytic removal of *s*-triazine ring substituents from the herbicide atrazine to yield cyanuric acid. Computational analyses indicated that pADP-1 encodes 104 putative open reading frames (ORFs), which are predicted to function in catabolism, transposition, and plasmid maintenance, transfer, and replication. Regions encoding transfer and replication functions of pADP-1 had 80 to 100% amino acid sequence identity to pR751, an IncPβ plasmid previously isolated from *Enterobacter aerogenes*. pADP-1 was shown to contain a functional mercury resistance operon with 99% identity to Tn5053. Complete copies of transposases with 99% amino acid sequence identity to TnpA from IS1071 and TnpA from *Pseudomonas pseudoalcaligenes* were identified and flank each of the *atzA*, *atzB*, and *atzC* genes, forming structures resembling nested catabolic transposons. Functional analyses identified three new catabolic genes, *atzD*, *atzE*, and *atzF*, which participate in atrazine catabolism. Crude extracts from *Escherichia coli* expressing AtzD hydrolyzed cyanuric acid to biuret. AtzD showed 58% amino acid sequence identity to TrzD, a cyanuric acid amidohydrolase, from *Pseudomonas* sp. strain NRRLB-12227. Two other genes encoding the further catabolism of cyanuric acid, *atzE* and *atzF*, reside in a contiguous cluster adjacent to a potential LysR-type transcriptional regulator. *E. coli* strains bearing *atzE* and *atzF* were shown to encode a biuret hydrolase and allophanate hydrolase, respectively. *atzDEF* are cotranscribed. AtzE and AtzF are members of a common amidase protein family. These data reveal the complete structure of a catabolic plasmid and show that the atrazine catabolic genes are dispersed on three disparate regions of the plasmid. These results begin to provide insight into how plasmids are structured, and thus evolve, to encode the catabolism of compounds recently added to the biosphere.

Many bacteria contain plasmids that carry genes functional in antibiotic resistance, virulence for animal or plant hosts, or the catabolism of diverse chemical compounds. While much has been learned since Lederberg's initial discovery of plasmids in 1952 (36), genomic approaches will further enhance our understanding of plasmid structure and evolution. Recently, the complete nucleotide sequences of approximately 90 bacterial and 10 archaeal plasmids have been obtained (5, 20, 29, 41, 46, 52, 59; [http://www.ncbi.nlm.nih.gov:80/PMGifs/Genomes/eub\\_p.html](http://www.ncbi.nlm.nih.gov:80/PMGifs/Genomes/eub_p.html)). However, most of the sequenced plasmids are relatively small, are used as vectors in molecular biology, or are of medical importance. The latter group of plasmids consist predominantly of those known to contain antibiotic resistance genes or encode virulence determinants associated with infectious diseases (5, 29, 52). In contrast, catabolic plasmids, which have been identified in many non-pathogenic soil bacteria (49), have been shown to transfer among bacteria, thus disseminating genes encoding the metabolism of environmentally relevant compounds (11). For example, plasmids encoding the catabolism of toluene, camphor,

naphthalene, and 2,4-dichlorophenoxyacetate are known (3, 12, 45, 64). Many of the genes involved in their respective catabolic pathways have been cloned and sequenced, but to date only one catabolic plasmid, pNL1, from *Sphingomonas aromaticivorans* strain F199 has been completely sequenced (46). This plasmid contains genes encoding enzymes for the metabolism of biphenyl, naphthalene, *m*-xylene, and *p*-cresol.

Metabolism of the herbicide atrazine has also been shown to be linked to catabolic plasmids. Mandelbaum et al. (38) isolated *Pseudomonas* sp. strain ADP, which metabolizes atrazine to carbon dioxide and ammonia. The first three enzymatic steps, encoded by the genes *atzA*, *atzB*, and *atzC*, transform atrazine to cyanuric acid (9, 15, 47). Cyanuric acid has been shown to be a common intermediate in the degradation pathways for melamine (2,4,6-triamino-*s*-triazine) and atrazine (21, 22, 47) in *Pseudomonas* sp. strain NRRLB-12227 and *Pseudomonas* sp. strain ADP, respectively (Fig. 1). However, while the hydrolysis of cyanuric acid in *Pseudomonas* sp. strain NRRLB-12227 proceeds through biuret and urea intermediates, the reactions involved in cyanuric acid degradation in *Pseudomonas* sp. strain ADP were not established.

The *atzA*, *atzB*, and *atzC* genes in *Pseudomonas* sp. strain ADP have been localized to an approximately 100 kb plasmid, pADP-1 (17), and DNA regions with homology to IS1071 have been shown to flank *atzA* (18). Recently, plasmid-localized

\* Corresponding author. Mailing address: Department of Soil, Water, and Climate, University of Minnesota, 1991 Upper Buford Circle, 439 Borlaug Hall, St. Paul, MN 55108. Phone: (612) 624-2706. Fax: (612) 625-6725. E-mail: [sadowsky@soils.umn.edu](mailto:sadowsky@soils.umn.edu).

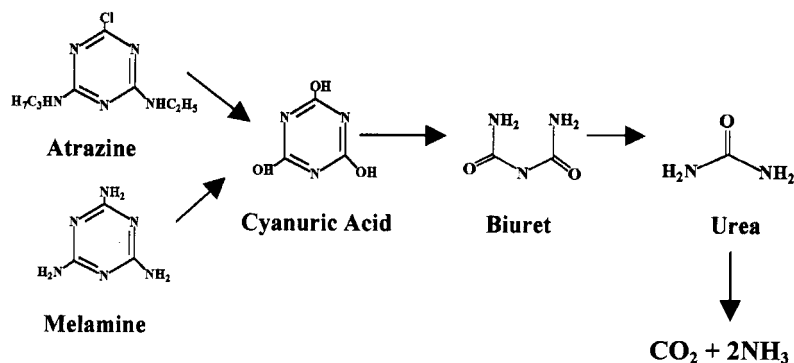


FIG. 1. Proposed pathway for the degradation of cyanuric acid by atrazine- and melamine-degrading bacteria. Cyanuric acid is hydrolyzed to biuret and is hypothesized to be subsequently hydrolyzed to urea, carbon dioxide, and ammonia.

genes homologous to the *atzA*, *atzB*, and *atzC* genes have been identified in different genera of atrazine-degrading bacteria isolated from geographically diverse locations (16; B. Martinez, M. de Souza, L. Wackett, and M. Sadowsky, Abstr. 99th Gen. Meet. Am. Soc. Microbiol., abstr. Q352, 1999). Since the atrazine catabolic genes have >99% sequence identity among different species of bacteria isolated independently from different continents, this suggests a recent evolution and dissemination of the *atzA*, *atzB*, and *atzC* genes.

To further our understanding about the assembly of the atrazine catabolic pathway and the accessory functions encoded by pADP-1, we undertook the complete sequencing and annotation of this plasmid. Sequence analysis revealed that the gene regions encoding plasmid replication, transfer, and maintenance functions of pADP-1 were nearly identical to those found on pR751, an IncP $\beta$  plasmid from *Enterobacter aerogenes*. Plasmid pADP-1 is predicted to encode 104 proteins. A functional mercury resistance operon is also present on pADP-1. Structural and functional studies showed that the genes encoding the initial reactions of atrazine catabolism are not organized in an operon, but are dispersed and flanked by transposases. Moreover, genes for the complete catabolism of cyanuric acid to CO<sub>2</sub> and NH<sub>3</sub> were localized to pADP-1.

#### MATERIALS AND METHODS

**Isolation of pADP-1 DNA.** The pADP-1 plasmid was introduced into *Escherichia coli* AD256 by conjugation as described previously (17). Cells were grown overnight in one-fourth-strength Luria-Bertani (LB) medium (48) containing 500  $\mu$ g of atrazine per ml. Cells were harvested by centrifugation at 8,000  $\times$  g for 10 min at 4°C. Large-scale plasmid DNA isolation preparations were done as described by Hirsch et al. (27), and pADP-1 was further purified using CsCl buoyant-density ultracentrifugation (48).

**Construction of pADP-1 shotgun library.** Plasmid pADP-1 DNA was nebulized using 4.4  $\times$  10<sup>4</sup> Pa of N<sub>2</sub> for 4.0 min and a nebulizer (IPT Medical Products Inc., Chicago, Ill.). The DNA ends were filled in, ligated into plasmid pUC18, and transferred to DH10B (Gibco-BRL, Grand Island N.Y.) as described previously (48). Clones containing inserts were picked randomly using the Genetix Q-Bot robot (Genetix Ltd., New Milton, United Kingdom) and stored in 96-well microtiter plates.

**DNA sequencing.** DNA templates from randomly selected shotgun clones were prepared from 3-ml overnight cultures grown in LB medium containing 50  $\mu$ g of ampicillin per ml using an AutoGene 740 DNA isolation system (Integrated Separation Systems, Framingham, Mass.). DNA from each preparation was dissolved in 80  $\mu$ l of sterile H<sub>2</sub>O and stored at -20°C until used. Plasmid DNA, 500 ng, was sequenced using M13 forward and reverse primers

and an ABI BigDye cycle sequencing kit (Applied Biosystems, Foster City, Calif.) and an ABI model 377 DNA sequencer (Applied Biosystems).

**Sequence assembly.** The Phred/Phrap/Consed sequence analysis software package was used to cross-match vector sequences and assemble the pADP-1 sequence into contigs (25). For gap closure, custom primers were designed from the ends of each contig in the pADP-1 sequence using Primer Designer software, version 2.01 (Scientific and Educational Software, State Line, Pa.). Primers were synthesized by Integrated DNA Technologies, Inc. (Coralville, Iowa). DNA fragments containing sequences necessary to close gaps between contigs were obtained by using the PCR high-fidelity *rTth* polymerase and purified plasmid pADP-1 DNA as a template. PCR was done using a Perkin-Elmer/Applied Biosystems XL Polymerase DNA amplification kit (PE/Applied Biosystems, Foster City, Calif.) and a PTC-100 thermocycler (MJ Research, Incline Village, Nev.). PCR products were purified using a Qiagen gel extraction kit (Qiagen, La Jolla, Calif.) and sequenced directly as described above. The pBluescript vector (Stratagene) was used to clone PCR products longer than 3 kb and facilitate sequencing.

**Analysis of ORFs.** The analysis of the open reading frames (ORFs) present in the pADP-1 sequence was completed using the web-based versions of GeneMark (7; <http://genemark.biology.gatech.edu/GeneMark/>), GeneMark.hmm (37; <http://genemark.biology.gatech.edu/GeneMark/hmmchoice.html>), Pfam (<http://pfam.wustl.edu/>), and the NCBI ORF Finder (<http://www.ncbi.nlm.nih.gov/gorf/gorf.html>) programs. ORFs that were consistently predicted by these programs were selected and met the following criteria: (i) the start codon was ATG, GTG, or TTG; (ii) the stop codon was TAA, TAG, or TGA; and (iii) the size of the ORF was between 150 and 5,000 bp. Start codon positions were assigned using manual identification of the Shine-Dalgarno sites within 15 bp of a potential start site. GeneMark.hmm (37) was also used to examine potential frameshifts leading to misidentification of ORFs. Those ORFs predicted to encode genes were analyzed further to determine their homology to proteins of known function using BLAST and BLASTP (<http://seqsim.ncgr.org/newBlast.html>).

**Cloning of the cyanuric acid hydrolase gene.** The putative cyanuric acid hydrolase gene, *atzD*, was cloned from pADP-1 using a PCR approach and primers CAAHF (5'-GCGGATCCTGCGTTCATCGACAGAG-3') and CAAHR (5'-GCGGATCCAGATGGCCTGTATCGCT-3'). The primers contained *Bam*HI restriction sites at each end to facilitate gene cloning. PCR was performed using a high-fidelity XL polymerase DNA amplification kit (PE/Applied Biosystems). Amplification of the 1.4-kb DNA fragment was achieved using the following conditions: 94°C for 1 min, and then 28 cycles consisting of 94°C for 15 s and 60°C for 5 min. A final extension of the PCR product was done at 72°C for 10 min. The PCR product was resolved on a 0.8% agarose gel, and the band was excised from the gel and purified using the Qiagen gel extraction kit (Qiagen, La Jolla, Calif.). The PCR product was cloned into the *Bam*HI site of pKT230 (4) using standard cloning procedures (48). Potential clones were screened for the insert by restriction enzyme digestions using *Bam*HI, and one clone, pBMZ1, was used for subsequent functional analyses.

**Cyanuric acid degradation assays.** To determine if the putative *atzD* gene encoded a cyanuric acid amidohydrolase, the hydrolysis of cyanuric acid by crude extracts of *E. coli* DH5 $\alpha$ (pBMZ1) and *E. coli* DH5 $\alpha$  was examined. Crude extracts were prepared as described previously (9). Reaction mixtures contained 10 mM potassium phosphate buffer (pH 7.2), 3 mM cyanuric acid (Sigma-Aldrich, St. Louis, Mo.), and 100  $\mu$ g of protein in a final reaction volume of 1.0

ml. Replicate reactions were incubated at 30°C and at various times terminated by heating at 95°C for 2 min. Samples were centrifuged at 14,000 × g for 10 min, filtered through 0.2-μm filters, and placed in vials for analysis by high-performance liquid chromatography (HPLC). The disappearance of cyanuric acid was monitored by HPLC analysis using an analytical Absorbosphere C<sub>18</sub> reverse-phase HPLC column (5-μm spherical packing; 250 by 4.6 mm) (Alltech Associates, Deerfield, Ill.). The isocratic mobile phase was 5 mM potassium phosphate buffer (pH 6.8) containing 5 mM dodecyltriethylammonium phosphate and Q12 ion pair cocktail (Regis Chemical Technologies, Morton Grove, Ill.) at a flow rate of 1.0 ml per min. Spectral data of the column eluent was acquired at 224 nm. Under these conditions, cyanuric acid eluted from the column at about 6.0 min and biuret at 3.3 min. The concentration of cyanuric acid in the sample analyzed was obtained by integrating peak areas at 224 nm. Biuret was resolved from reaction mixtures using an Absorbosphere C<sub>18</sub> reverse-phase HPLC column as described above, and its identity was confirmed by direct insertion mass spectroscopy with a Kratos MS25 mass spectrometer (Ramsey, N.J.) using electron impact ionization at 70 eV.

**Biuret degradation assays.** Plate-clearing, ammonia release, thin-layer chromatography (TLC), and HPLC assays were used to determine if ORF101 (*atzE*) encoded biuret hydrolase activity. One clone from the pADP-1 sequencing library, p11A07, containing a complete copy of ORF101 was used for these analyses. For the plate-clearing assays, 500 μl of an *E. coli*(p11A07) culture (optical density at 600 nm [OD<sub>600</sub>] = 1.0) was placed onto the surface of one-fourth-strength LB medium plates containing 60 mM sodium phosphate buffer and 4,000 μg of biuret per ml. Plates were incubated at 37°C for up to 1 week. The appearance of clearing zones surrounding cell growth indicated biuret degradation.

Ammonia release assays were done in 50 mM sodium phosphate buffer (pH 8.0) containing 3 mM biuret and cell extract (1 mg of protein) from *E. coli* (p11A07). Reaction mixtures were incubated at 30°C for 6 h. Samples were taken at several time points, and the reactions were stopped by addition of 1 N H<sub>2</sub>SO<sub>4</sub>. For urea-coupled assays, reaction mixtures were treated with 100 U of type III jack bean urease (Sigma, St. Louis, Mo.) during incubations. Analysis of released ammonia was determined using the Berthelot reactions described by Weatherburn (61) with the following modifications: 500 μl of the reaction mixture was treated with 200 μl of 0.3 M Na<sub>2</sub>WO<sub>4</sub> and 200 μl of 1 N sulfuric acid to precipitate proteins. The samples were mixed and centrifuged for 5 min at 14,000 × g, and 500 μl of the supernatant was treated with 1.5 ml of solution A (1% phenol and 0.005% sodium nitroprusside in water) and 2.0 ml of solution B (0.5% NaOH and 0.84% sodium hypochlorite in water). Reactions were incubated at room temperature for 1 h, and the resulting indophenol was monitored at 630 nm.

The degradation of biuret was also examined by HPLC analyses. Cell extracts of *E. coli* DH5α(p11A07) and *E. coli* DH5α(pUC18) were prepared as described previously (9). Reaction mixtures containing 50 mM sodium phosphate buffer (pH 7.0), 0.6 mM biuret, and cell extract (1 mg of protein), in a final volume of 10 ml, were incubated at 30°C. Reactions were terminated by heating at 95°C for 3 min. Samples were centrifuged at 14,000 × g for 10 min, filtered through 0.2-μm filters, and analyzed by HPLC. The disappearance of biuret was followed by using a Waters IC-Pak A HC anion-exchange column (150 mm by 4.6 mm; Waters Corp., Milford, Mass.). The isocratic mobile phase consisted of 5 mM sodium phosphate buffer (pH 7.0) at a flow rate of 0.5 ml per min (35). Spectral data of the column eluent were collected at 200 nm. Under these conditions, urea eluted after 3.9 min and biuret eluted after 5.0 min. The concentration of biuret was obtained by integrating peak areas at 200 nm.

TLC analyses were performed as described by Radosevich (44) to detect the products of biuret degradation. Reaction mixtures containing 1 mM sodium phosphate buffer (pH 8.0), 3 mM biuret, and cell extract (1 mg of protein), in a final reaction volume of 10 ml, were incubated overnight at 30°C. Samples of the reaction mixture (1.0 ml) were evaporated to dryness using a SpeedVac concentrator (Savant Instruments Inc., Farmingdale, N.Y.) and resuspended in 25 μl of NH<sub>4</sub>OH. Samples were chromatographed on Cellulose 300, F-254 TLC plates (Selecto Scientific, Suwanee, Ga.) using a mobile phase consisting of 40% *t*-butyl alcohol, 30% methyl ethyl ketone, 10% ammonium hydroxide, and 20% water. Standards and reactions products were visualized by spraying the plate with a solution containing 1 g of 4-diethylaminobenzaldehyde in 75 ml of methanol and 25 ml of concentrated HCl.

**Allophanate degradation assays.** Ammonia release, HPLC, and urea agar plate assays were done to determine if ORF102 (*atzF*) encoded allophanate hydrolase activity. For these studies, a clone from the pADP-1 sequencing library, p14D12, containing only the complete copy of ORF102 was used. To test for urea hydrolysis, 500 μl of *E. coli*(p14D12) and *E. coli*(pUC18) cultures (OD<sub>600</sub> = 1.0) were spotted onto the surface of urea agar (Difco, Detroit, Mich.).

The cultures were incubated for up to 1 week at 37°C, and urea hydrolysis was monitored by observing a change in the color of the medium, indicating an increase in pH due to urea hydrolysis.

Ammonia release assays were done to determine if urea or allophanate was a substrate for ORF102. These studies were done using cell extracts from *E. coli* (p14D12) and *E. coli*(pUC18). Ultrapure urea was obtained from Gibco-BRL (Grand Island, N.Y.). Potassium allophanate was synthesized from ethyl allophanate (Fisher Scientific, Pittsburgh, Pa.) using the following method. Twenty millimoles of ethyl allophanate was mixed with 25 mmol of KOH and heated at 40°C for 3 h. The mixture was dissolved in 250 ml of 100% ethanol and 50 ml of diethylether. The reaction mixture was incubated at 4°C for 8 h, filtered, and dried in a desiccator until ready to use. The ammonia release procedure described above was used with the following modifications: reactions were done in 10 mM sodium phosphate buffer (pH 8.0) containing 4 mM potassium allophanate or 3 mM urea, and each sample contained 32 μg of protein from cell extracts. Reactions were terminated by adding 200 μl of 1 N sulfuric acid.

HPLC analyses done to detect allophanate degradation were performed essentially as described above except that the isocratic mobile phase consisted of 10 mM sodium phosphate buffer (pH 8.0). Samples were assayed in 10 mM sodium phosphate buffer (pH 8.0) containing 4 mM potassium allophanate and 32 μg of protein. Reactions were terminated by adding 4 μl of 3 M NaOH. Under these conditions, allophanate eluted after 11.2 min.

**RT-PCR analyses.** RNA was isolated from exponentially growing *Pseudomonas* sp. strain ADP cells using the diethyl polycarbonate (DEPC) of Summers (56). RNA samples were treated with 10 U of RNase-free DNase (Takara Biomedical Group, Shiga, Japan) for 1 h at 37°C, extracted twice with phenol-chloroform, and ethanol precipitated. The resulting RNA was quantified spectrophotometrically.

Reverse transcriptase PCR (RT-PCR) reactions were done using the GeneAmp RNA PCR kit (PE/Applied Biosystems, Branchburg, N.J.). Reverse transcriptase reactions were carried out with 500 ng of RNA and random hexamer primers using the following protocol: 10 min at 25°C, 15 min at 42°C, 5 min at 99°C, and 5 min at 5°C. The complete reverse transcriptase reaction mixture was used as the template for cDNA PCR. This was done using primer pairs specific for the DNA region upstream of *atzD* and ORF101 (*atzE*) [5'-*atzD*-f (5'-CGGC GTACCTAACTCGT-3') and ORF101-r (5'-GCGTATGGAACCGTTGG-3')] and the region between *atzE* and *atzF* [*atzE*-f (5'-GCCAGCGAAGTCGTCAT-3') and *atzF*-r (5'-TCTGTACCGCGGCATA-3')]. Since a single mRNA from *atzD* to *atzF* would be approximately 5.2 kb and difficult to amplify, two primer pairs were used to amplify overlapping cDNA regions. The following PCR protocol was used: 1 min at 94°C, 20 cycles of 15 s at 94°C and 5 min at 63°C, and 18 cycles at 95°C for 15 s and 63°C for 5 min, with an extension of 15 s per cycle. The PCR mixture was subjected to a final extension of 72°C for 10 min. Reaction products were separated by horizontal gel electrophoresis on 0.85% agarose, stained, and photographed under UV light.

**Mercury resistance analyses.** The functionality of the putative mercury resistance operon in pADP-1 was determined by disk (62) and mercuric reductase activity assays (23). The disk assay was used to determine if the presence of pADP-1 allowed recipient bacteria to grow in media containing different concentrations of HgCl<sub>2</sub>. *E. coli* strains AD256 (17), AD256(pADP-1) (17), S17-1 (53) and S17-1(pADP-1) were grown to mid-log phase in LB medium containing 100 μg of atrazine per ml. Aliquots, 100 μl, of each strain were spread-plated onto the surface of LB plates, and filter disks with 0, 50, 100, 150, 200, 250, and 300 μg of HgCl<sub>2</sub> per ml were overlaid onto the inoculated medium. Plates were incubated overnight at 37°C, and sensitivity to Hg was determined by the size of the growth inhibition zones surrounding the disks. Mercuric reductase activity was determined by monitoring Hg-dependent oxidation of NADPH. *E. coli* strains AD256(pADP-1) and S17-1(pADP-1) were grown in 100 ml of LB liquid medium containing 10 μM HgCl<sub>2</sub> (Sigma-Aldrich, St. Louis, Mo.) to mid-log phase (OD<sub>600</sub> = 0.5), after which an additional 20 μM HgCl<sub>2</sub> was added to the medium. Cultures were grown for an additional 1 h and centrifuged at 10,000 × g, and cell pellets were washed twice in 10 mM potassium phosphate buffer (pH 7.4). Cells were resuspended in 10 ml of potassium phosphate buffer (pH 7.4), and crude cell extracts were prepared as previously described (9). Reaction mixtures contained 150 μM NADPH, 200 μM disodium EDTA, 1.0 mM β-mercaptoethanol, 2 μM flavin adenine dinucleotide, and 0.05 mg of total cell protein in 50 mM sodium phosphate buffer (pH 7.2), and were preincubated at 4°C for 10 min. Reactions were initiated by the addition of 100 μM HgCl<sub>2</sub>. The oxidation of NADPH was followed by monitoring the decrease in absorbance at 340 nm for 10 min. Assays were done in triplicate.

**Nucleotide sequence accession number.** The complete nucleotide sequence of pADP-1 from *Pseudomonas* sp. strain ADP has been deposited with GenBank as accession number U66917.

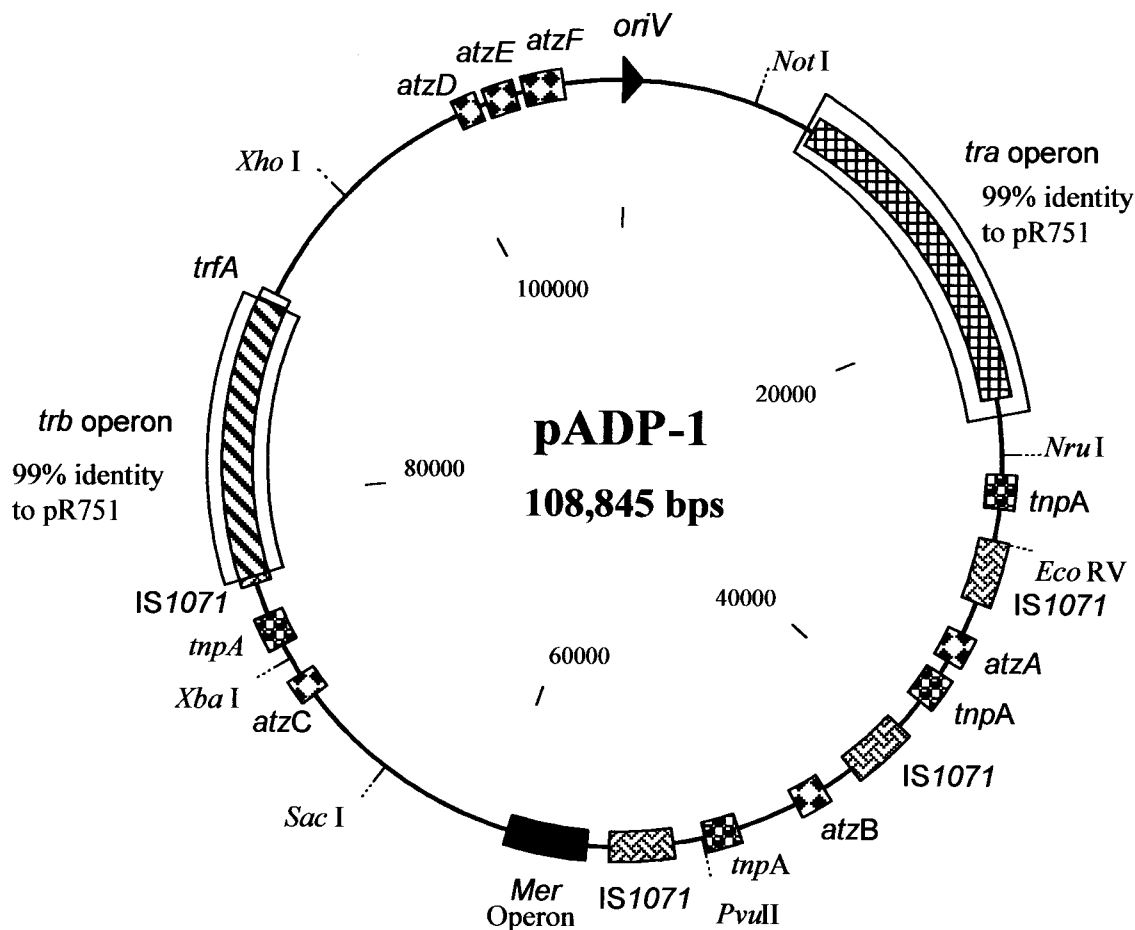


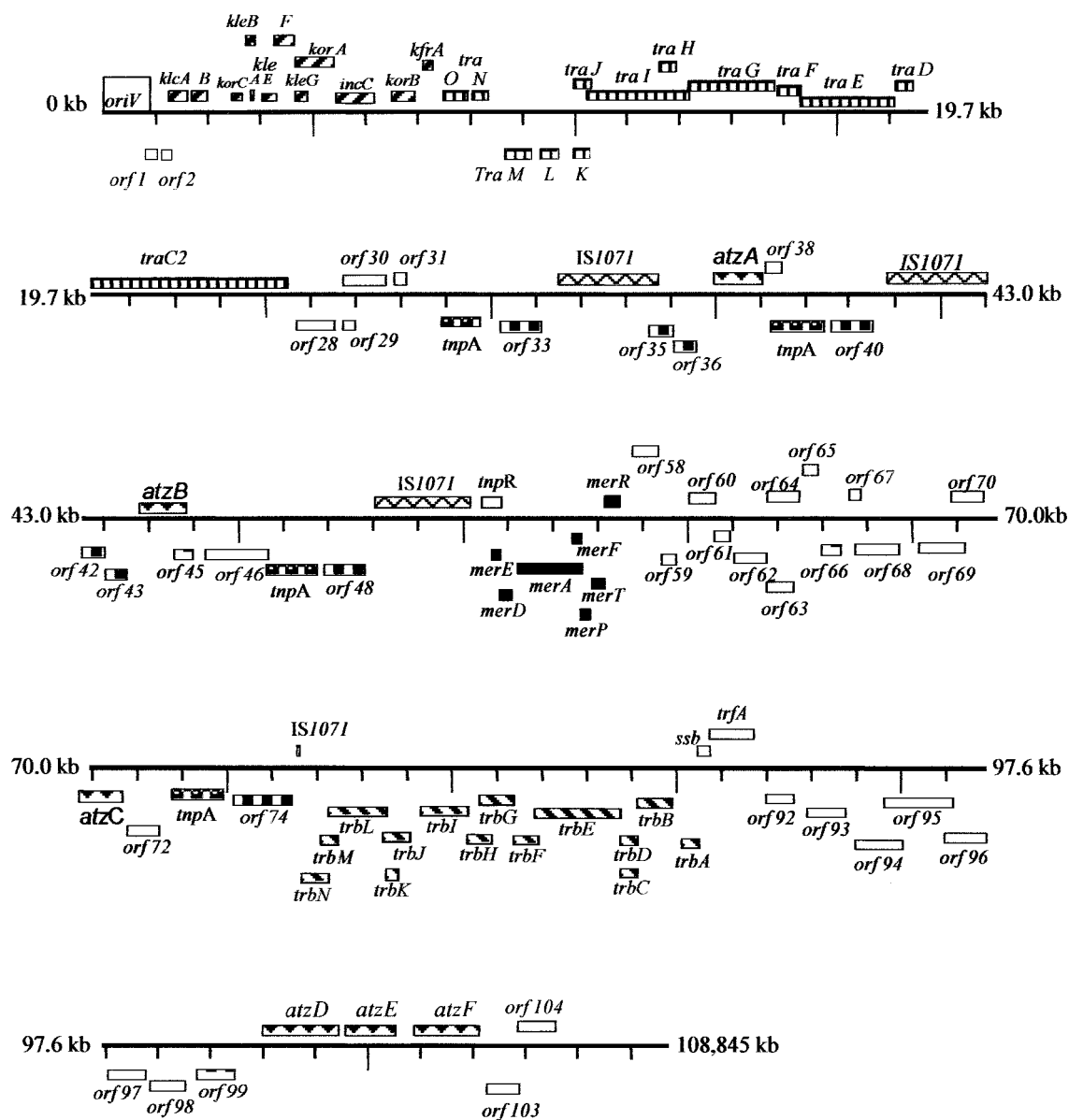
FIG. 2. Physical circular map of the catabolic plasmid pADP-1 from *Pseudomonas* sp. strain ADP. The map positions of selected restriction sites, genes, and operons on pADP-1 are indicated. Regions with 99% identity to the *tra* and *trb* operons of plasmid pR751 are boxed. Genes involved in atrazine catabolism are indicated. Copies of similar putative transposons have the same shading.

## RESULTS

**Nucleotide sequence, physical map, and genetic organization of pADP-1.** The atrazine catabolic plasmid pADP-1 is 108,845 bp, with an overall G+C content of 62.6 mol%. This value is within the range of those found in several genera of gram-negative soil bacteria, including *Pseudomonas* and *Alcaligenes* strains (28, 40). A circular physical map of pADP-1 is shown in Fig. 2. The assembly of pADP-1 was verified by using restriction enzyme analyses and PCR (data not shown). This plasmid contains a classical IncP $\beta$  backbone that consists of two regions involved in plasmid conjugation (the *tra* and *trb* operons), an origin of replication (*oriV*), and a region involved in plasmid control, stable inheritance, and partitioning. The nucleotide sequence of the pADP-1 backbone is 80 to 100% identical to the backbone of the archetype IncP $\beta$  plasmid R751 except for *kleG*. The main catabolic region of pADP-1 lies outside the *trb* and *tra* operons. This region contains the first three genes necessary for the degradation of atrazine, *atzA*, *atzB*, and *atzC*. In addition, the region contains a mercury resistance operon and several insertion sequence elements. Restriction enzyme analysis of pADP-1 showed that the catabolic region of this plasmid contains numerous restriction sites, while only a few enzymes cut the backbone.

**Analyses of ORFs.** A total of 104 ORFs were identified in the pADP-1 sequence using GeneMark, GeneMark.hmm, and NCBI ORF Finder (Fig. 3). All three ORF-finding programs identified the same ORFs. Based on significant similarities to proteins of known function, putative functions were assigned to a majority of the ORFs (Table 1); 15% of the ORFs were predicted to be involved in catabolism, 15% were predicted to be involved in transposition, 5% encode putative transporters, 3% are putative transcriptional regulators, 13% are proteins involved in general metabolism, and 39% are proteins necessary for plasmid maintenance, transfer, and replication. Several ORFs (8%) had >38% amino acid identity to hypothetical proteins, and 2% had no significant homology to any known proteins in databases. The first ORF after the origin of replication, *oriV*, was arbitrarily assigned as ORF1 (Table 1 and Fig. 3). More detailed descriptions of many of the ORFs and genes on pADP-1 are found below.

**Similarities and differences between pADP-1 and pR751.** Sequence analyses revealed that the regions of pADP-1 containing replication, basic transfer, and maintenance functions were nearly identical to gene regions encoding these functions in the IncP $\beta$  plasmid pR751 from *Enterobacter aerogenes*. The *tra* and *trb* operons of pADP-1 and pR751 contain genes nec-



**Symbols:** *tra* genes, atrazine catabolic genes, IS1071, IS801-like transposase genes, mercury resistance genes, *pdhL* and *pdhB* homologs, potential regulatory genes, *trb* genes, genes involved in plasmid replication and maintenance.

FIG. 3. Linear map showing graphical representation of ORFs present on the pADP-1 sequence. Boxes above the lines refer to ORFs on the top strand, while those below the line are from the complementary strand. Genes of the same type (operons, insertion sequence [IS] elements, and catabolic genes) have similar shading, and ORFs with putative functions are listed by their numbers. ORFs and genes have been numbered relative to the origin of replication (*oriV*). Distance between tick marks is 1.3 kb.

essary for plasmid transfer and replication (59). In addition, the origin of replication and the *IncC*, *KorA*, *KorB*, and *Klc* proteins, which are involved in the regulation of replication and maintenance of pR751, are highly conserved in pADP-1 (Table 1). These observations suggest that pADP-1 and pR751 have a common ancestor.

Despite having similarity in backbone structure, the regions

between *oriV* and *trfA* and between *trb* and *tra* of plasmids pR751 and pADP-1 are different. In pR751, two transposons, Tn4321 and Tn402/Tn5090, are located in the regions between *oriV-trfA* and *trb-tra*, respectively; these transposons are not present in pADP-1. Moreover, in pADP-1 two complete copies of a transposase similar to *TnpA* from IS801 flank the region between *trb* and *tra*. In pADP-1, this 52-kb region resembled a

TABLE 1. Localization and predicted functions of ORFs in pADP-1

ORF no.	Positions (bp) <sup>a</sup>	Function of closest relative	Source microorganism	No. of amino acids, pADP-1/relative <sup>c</sup>	% Amino acid identity <sup>d</sup>	GenBank accession no.	E value <sup>e</sup>
1	869–1183 c	Hypothetical protein—no significant homology to others	N/A <sup>b</sup>	N/A	N/A	N/A	N/A
2	1180–1461 c	Hypothetical protein—no significant homology to others	N/A	N/A	N/A	N/A	N/A
3	1618–2046 d	Protein involved in stable inheritance (KlcA)	<i>Enterobacter aerogenes</i> pR751	142/142	100 (142/142)	AAC64430.1	1.00E–77
4	2098–2517 d	Protein involved in stable inheritance (KlcB)	<i>Enterobacter aerogenes</i> pR751	139/371	91 (106/116)	AAC64429.1	3.00E–55
5	3427–3684 d	Transcriptional repressor (KorC)	<i>Enterobacter aerogenes</i> pR751	85/84	92 (78/84)	AAC64428.1	8.00E–41
6	3844–4080 d	Protein involved in stable inheritance (KlcA)	<i>Enterobacter aerogenes</i> pR751	78/78	100 (78/78)	AAC64427.1	2.00E–38
7	4139–4354 d	Protein involved in stable inheritance (KlcB)	<i>Enterobacter aerogenes</i> pR751	71/71	100 (71/71)	AAC64426.1	1.00E–34
8	4442–4828 d	Protein involved in stable inheritance (KlcE)	<i>Enterobacter aerogenes</i> pR751	128/109	82 (90/109)	AAC64425.1	7.00E–48
9	4830–5360 d	Protein involved in stable inheritance (KlcF)	<i>Enterobacter aerogenes</i> pR751	176/97	91 (88/96)	AAC64424.1	2.00E–47
10	5104–5367 d	Protein involved in stable inheritance (KlcG)	<i>Enterobacter aerogenes</i> pR751	87/89	43 (37/86)	AAC64423.1	2.00E–05
11	5461–6537 d	Inclusion membrane protein (IncC)	<i>Enterobacter aerogenes</i> pR751	358/358	100 (358/358)	AAC64421.1	0.00
12	5474–5776 d	Transcriptional repressor (KorA)	<i>Enterobacter aerogenes</i> pR751	100/100	100 (100/100)	AAC64422.1	3.00E–50
13	6534–7583 d	Transcriptional repressor protein (KorB)	<i>Enterobacter aerogenes</i> pR751	349/349	99 (347/349)	AAC64419.1	0.00
14	7763–8794 d	Transcriptional regulator (KfrA)	<i>Enterobacter aerogenes</i> pR751	343/343	99 (341/343)	AAC64418.1	1.00E–180
15	8965–9312 d	TraO protein	<i>Enterobacter aerogenes</i> pR751	115/115	99 (14/115)	AAC64417.1	2.00E–59
16	9341–9994 d	TraN protein	<i>Enterobacter aerogenes</i> pR751	217/217	96 (210/217)	AAC64416.1	1.00E–112
17	10197–10637 c	Essential transfer protein (TraM)	<i>Enterobacter aerogenes</i> pR751	146/146	100 (146/146)	AAC64481.1	2.00E–74
18	10637–11362 c	Transfer origin protein (TraL)	<i>Enterobacter aerogenes</i> pR751	241/241	99 (240/241)	AAC64480.1	1.00E–135
19	11362–11760 c	<i>oriT</i> binding protein (TraK)	<i>Enterobacter aerogenes</i> pR751	132/132	100 (132/132)	AAC64479.1	9.00E–75
20	12134–12508 d	<i>oriT</i> binding protein (TraJ)	<i>Enterobacter aerogenes</i> pR751	124/130	87 (113/129)	AAC64478.1	1.00E–54
21	12543–14783 d	DNA relaxase (TraI)	<i>Enterobacter aerogenes</i> pR751	747/747	99 (743/747)	AAC64475.1	0.00E 00
22	14089–14481 d	Relaxosome stabilization protein (TraH)	<i>Enterobacter aerogenes</i> pR751	130/130	100 (130/130)	AAC64476.1	1.00E 73
23	14780–16693 d	DNA transport protein (TraG)	<i>Enterobacter aerogenes</i> pR751	637/637	100 (636/637)	AAC64474.1	0.00
24	16690–17226 d	Maturation peptidase (TraF)	<i>Enterobacter aerogenes</i> pR751	178/178	100 (178/178)	AAC64473.1	3.00E–98
25	17238–19301 d	DNA topoisomerase (TraE)	<i>Enterobacter aerogenes</i> pR751	687/687	85 (593/687)	AAC64472.1	0.00
26	19323–19712 d	Unknown function (TraD)	<i>Enterobacter aerogenes</i> pR751	129/129	100 (129/129)	AAC64471.1	7.00E–69
27	19716–24062 d	DNA replication primase (TraC)	<i>Enterobacter aerogenes</i> pR751	1,448/1,448	99 (1,446/1,448)	AAC64468.1	0.00
28	24327–25175 c	Cointegrate formation and resolution protein (IstB)	<i>Ralstonia eutropha</i> NH9	282/264	69 (170/245)	BAA33970.1	1.00E–90
29	25159–25416 c	Cointegrate formation and resolution protein (IstA)	<i>Ralstonia eutropha</i> NH9	84/518	44 (34/76)	BAA33969.1	5.00E–09
30	25315–26307 d	Conserved hypothetical protein	<i>Synechocystis</i> sp. strain 6803	353/535	46 (131/283)	BAA10081.1	7.00E–66
31	26288–26764 d	Putative cytosine deaminase	<i>A. avenae</i> subsp. <i>citulli</i> 12227	158/158	100 (158/158)	AAK00500.1	8.00E–82
32	27514–29061 c	Transposase similar to TnpA from IS801	<i>P. pseudoalcaligenes</i> JS45	515/515	99 (514/515)	AAB94124.1	1.00E–150
33	29170–30372 c	Dihydroliipoamide dehydrogenase (PdhL)	<i>Ralstonia eutropha</i> H16	400/594	68 (276/401)	AAA21600.1	1.00E–154
34	30521–33436 d	Transposase from IS1071	<i>Alcaligenes</i> sp. strain BR60	971/970	99 (971/971)	AAA70396.1	0.00
35	33549–34253 c	Dihydroliipoamide dehydrogenase (PdhL)	<i>Ralstonia eutropha</i> H16	234/594	63 (145/229)	AAA21600.1	9.00E–75
36	34270–34920 c	Dihydroliipoamide acetyltransferase (PdhB)	<i>Ralstonia eutropha</i> H16	216/553	82 (174/212)	AAA21599.1	3.00E–99
37	34964–36388 d	Atrazine chlorohydrolase (AtzA)	<i>Pseudomonas</i> sp. strain ADP	474/474	100 (474/474)	AAC64663.1	0.00
38	36392–36856 d	Amidase	<i>R. rhodochrous</i> J1	154/515	46 (70/154)	BAA03744.1	7.00E–28
39	37037–38584 c	Transposase similar to TnpA from IS801	<i>P. pseudoalcaligenes</i> JS45	515/515	99 (514/515)	AAB94124.1	0.00
40	38693–39895 c	Dihydroliipoamide dehydrogenase (PdhL)	<i>Ralstonia eutropha</i> H16	400/594	68 (276/401)	AAA21600.1	1.00E–154
41	40043–42959 d	Transposase from IS1071	<i>Alcaligenes</i> sp. strain BR60	971/970	99 (971/971)	AAA70396.1	0.00
42	43072–43776 c	Dihydroliipoamide dehydrogenase (PdhL)	<i>Ralstonia eutropha</i> H16	234/594	63 (145/229)	AAA21600.1	9.00E–75
43	43793–44443 c	Dihydroliipoamide acetyltransferase (PdhB)	<i>Ralstonia eutropha</i> H16	216/553	82 (174/212)	AAA21599.1	1.00E–100
44	44487–45932 d	Hydroxyatrazine hydrolase (AtzB)	<i>Pseudomonas</i> sp. strain ADP	481/481	100 (481/481)	AAC45138.1	0.00
45	45919–46494 c	Transcriptional regulator Tet/Acr family	<i>Aquifex aeolicus</i> VF5	191/192	30 (27/90)	AAG07881.1	2.00E–06
46	46883–48223 c	Conserved hypothetical protein	<i>D. radiodurans</i> R1	446/464	43 (198/457)	AAF12190.1	2.00E–89
47	48776–50323 c	Transposase similar to TnpA from IS801	<i>P. pseudoalcaligenes</i> JS45	515/515	100 (515/515)	AAB94124.1	0.00
48	50432–51688 c	Dihydroliipoamide dehydrogenase (PdhL)	<i>Ralstonia eutropha</i> H16	319/594	69 (236/341)	AAA21600.1	1.00E–129
49	51784–54699 d	Transposase from IS1071	<i>Alcaligenes</i> sp. strain BR60	971/970	99 (969/971)	AAA70396.1	0.00
50	55067–55681 d	Resolvase from Tn5053 transposon	<i>Xanthomonas</i> sp. strain W17	204/204	99 (203/204)	AAA98330.1	1.00E–110
51	55734–55970 c	MerE protein from Tn5053 transposon	<i>Xanthomonas</i> sp. strain W17	78/78	100 (78/78)	AAA98328.1	4.00E–40
52	55967–56332 c	Mercury coregulator protein from Tn5053 (MerD)	<i>Xanthomonas</i> sp. strain W17	121/121	100 (121/121)	AAA98327.1	9.00E–63
53	56348–57994 c	Mercury reductase from Tn5053 (MerA)	<i>Xanthomonas</i> sp. strain W17	548/548	99 (547/548)	AAA98326.1	0.00
54	57991–58236 c	Mercury ion transport protein from Tn5053 (MerT)	<i>Xanthomonas</i> sp. strain W17	81/81	100 (81/81)	AAA98325.1	1.00E–30
55	58239–58514 c	Periplasmic mercury ion binding (MerP)	<i>Xanthomonas</i> sp. strain W17	91/91	100 (91/91)	AAA98324.1	8.00E–45
56	58530–58880 c	Mercury ion transport protein	<i>Xanthomonas</i> sp. strain W17	116/116	100 (116/116)	AAA98323.1	2.00E–63
57	58952–59386 d	Mercury regulatory protein (MerR)	<i>Xanthomonas</i> sp. strain W17	144/144	100 (144/144)	AAA98322.1	9.00E–78
58	59783–60556 d	Conserved hypothetical protein	<i>P. aeruginosa</i> PAO1	257/205	61 (127/205)	AAG06457.1	2.00E–68
59	60661–61119 c	Conserved hypothetical protein	<i>P. aeruginosa</i> PAO1	152/152	86 (98/113)	AAG03518.1	8.00E–53
60	61471–62265 d	Putative glutamine amidotransferase	<i>P. aeruginosa</i> PAO1	264/250	43 (107/248)	AAG03686.1	2.00E–54
61	62296–62769 c	Conserved hypothetical protein	<i>P. aeruginosa</i> PAO1	157/166	64 (90/128)	AAG03517.1	9.00E–48
62	62824–63771 c	Conserved hypothetical protein; glycerol sensor protein homolog	<i>P. aeruginosa</i> PAO1	315/287	62 (183/274)	AAG05365.1	2.00E–89
63	63790–64593 c	Conserved hypothetical protein	<i>P. aeruginosa</i> PAO1	267/278	61 (175/286)	AAG03555.1	3.00E–95
64	63796–64755 d	Mutator protein (MutT)	<i>Synechocystis</i> sp. strain 6803	319/136	32 (30/94)	BAA16660.1	4.08E–02
65	64864–65307 d	Short-chain dehydrogenase	<i>P. aeruginosa</i> PAO1	147/265	66 (97/147)	AAG08217.1	3.00E–48
66	65433–65999 c	Putative transcriptional regulator	<i>P. aeruginosa</i> PAO1	188/186	67 (126/188)	AAG08216.1	9.00E–64
67	66253–66582 d	Dihydroliipoamide dehydrogenase 3	<i>P. aeruginosa</i> PAO1	109/467	78 (85/109)	AAG08214.1	3.00E–54
68	66429–67739 c	Putative transposase	<i>A. pasteurianus</i> 11380	436/461	45 (130/284)	BAA00934.1	6.00E–60

Continued on following page

TABLE 1—Continued

ORF no.	Positions (bp) <sup>a</sup>	Function of closest relative	Source microorganism	No. of amino acids, pADP-1/relative <sup>c</sup>	% Amino acid identity <sup>d</sup>	GenBank accession no.	E value <sup>e</sup>
69	67797–68942 c	Mg/citrate secondary transporter	<i>Bacillus subtilis</i> 6GM	381/433	21 (82/386)	AAC44564.1	3.00E–05
70	69053–70021 d	Transposase	<i>R. solanacearum</i> PS68	322/321	66 (211/318)	AAD49338.1	1.00E–117
71	70219–71430 c	N-Isopropylammelide isopropylamino hydrolase (AtzC)	<i>Pseudomonas</i> sp. strain ADP	403/403	100 (403/403)	AAB96621.1	0.00
72	71488–72447 c	Carbamoyl phosphate synthetase	<i>Pyrococcus abassy</i> GE5	319/314	51 (162/315)	AAF23075.1	2.00E–86
73	72897–74444 c	Transposase similar to TnpA from IS801	<i>P. pseudoalcaligenes</i> JS45	515/515	100 (515/515)	AAB94124.1	0.00
74	74260–75759 c	Dihydrolypoamide dehydrogenase (PdhL)	<i>Ralstonia eutropha</i> H16	499/594	68 (228/335)	AAA21600.1	1.00E–122
75	75908–76264 d	Transposase from IS1071	<i>Alcaligenes</i> sp. strain BR60	118/970	100 (118/118)	AAA70396.1	6.00E–60
76	76280–76915 c	Mating pair formation protein (TrbN)	<i>Enterobacter aerogenes</i> pR751	211/211	99 (209/211)	AAC64455.1	1.00E–120
77	76929–77516 c	Mating pair formation protein (TrbM)	<i>Enterobacter aerogenes</i> pR751	195/196	90 (178/196)	AAC64454.1	1.00E–95
78	77534–79252 c	DNA topoisomerase (TrbL)	<i>Enterobacter aerogenes</i> pR751	572/572	99 (570/572)	AAC64453.1	0.00
79	79263–79490 c	Protein involved in plasmid entry/exclusion (TrbK)	<i>Enterobacter aerogenes</i> pR751	75/75	97 (73/75)	AAC64452.1	4.00E–37
80	79500–80264 c	Mating pair formation protein (TrbJ)	<i>Enterobacter aerogenes</i> pR751	254/254	100 (254/254)	AAC64451.1	1.00E–139
81	80285–81706 c	Mating pair formation protein (TrbI)	<i>Enterobacter aerogenes</i> pR751	473/473	99 (471/473)	AAC64450.1	0.00
82	81711–82199 c	Mating pair formation protein (TrbH)	<i>Enterobacter aerogenes</i> pR751	162/162	99 (161/162)	AAC64449.1	3.00E–86
83	82202–83122 c	Mating pair formation protein (TrbG)	<i>Enterobacter aerogenes</i> pR751	306/306	99 (303/306)	AAC64448.1	1.00E–173
84	83119–83901 c	Mating pair formation protein (TrbF)	<i>Enterobacter aerogenes</i> pR751	260/260	99 (258/260)	AAC64447.1	1.00E–150
85	83898–86456 c	Mating pair formation protein (TrbE)	<i>Enterobacter aerogenes</i> pR751	852/852	99 (847/852)	AAC64446.1	0.00
86	86453–86764 c	Mating pair formation protein (TrbD)	<i>Enterobacter aerogenes</i> pR751	103/103	98 (101/103)	AAC64445.1	1.00E–53
87	86768–87232 c	Mating pair formation protein (TrbC)	<i>Enterobacter aerogenes</i> pR751	154/154	99 (152/154)	AAC64444.1	6.00E–82
88	87249–88211 c	ATPase autophosphorylase (TrbB)	<i>Enterobacter aerogenes</i> pR751	320/320	99 (319/320)	AAC64443.1	0.00
89	88521–88883 c	Regulatory protein for mating pair formation (TrbA)	<i>Enterobacter aerogenes</i> pR751	121/121	98 (118/120)	AAC64442.1	4.00E–61
90	88997–89338 d	Single-strand DNA-binding protein (SSB)	<i>Enterobacter aerogenes</i> pR751	113/113	100 (113/113)	AAC64441.1	2.00E–61
91	89488–90399 d	DNA-binding protein for plasmid replication (TrfA)	<i>Enterobacter aerogenes</i> pR751	303/407	96 (292/304)	AAA17040.1	1.00E–162
92	90795–92165 c	Putative transposase	<i>Streptococcus pyogenes</i> AP1	456/410	29 (110/378)	AAC38767.1	6.00E–33
93	92490–93821 c	Cytosine deaminase	<i>R. leguminosarum</i> T24	443/450	32 (141/428)	AAB17512.1	5.00E–46
94	94005–94928 c	Putative permease of ABC transporter	<i>P. aeruginosa</i> PAO1	327/308	55 (171/306)	AAG03528.1	3.00E–86
95	94918–96039 c	Putative permease of ABC transporter	<i>P. aeruginosa</i> PAO1	373/365	52 (187/357)	AAG03527.1	1.00E–97
96	96026–97648 c	Putative ATP-binding domain of ABC transporter	<i>P. aeruginosa</i> PAO1	540/523	58 (289/510)	AE004451.7	1.00E–154
97	97655–98737 c	Conserved hypothetical protein	<i>P. aeruginosa</i> PAO1	360/365	53 (184/347)	AAG03536.1	2.00E–99
98	98776–99834 c	Conserved hypothetical protein	<i>P. aeruginosa</i> PAO1	352/277	38 (98/256)	AAG03623.1	2.00E–40
99	99885–100853 c	Putative transcriptional regulator (LysR family)	<i>R. leguminosarum</i> T24	322/300	39 (116/295)	AAB17511.1	4.00E–44
100	101053–102144 d	Cyanuric acid amidohydrolase (AtzD)	<i>Pseudomonas</i> sp. strain 12227	363/370	58 (212/363)	AAC61577.1	1.00E–110
101	102427–103800 d	Nicotinamidase/pyrazinamidase	<i>Mycobacterium smegmatis</i> MC55	457/468	37 (171/454)	AAC77368.1	5.00E–64
102	104283–106100 d	Urea amidolyase	<i>Saccharomyces cerevisiae</i>	605/1835	44 (254/572)	CAA85172.1	1.00E–126
103	106158–106941 c	Similar to OrfQ	<i>Pseudomonas</i> sp. strain KHP41	260/349	36 (70/190)	CAA67456.1	2.00E–24
104	107219–108286 d	Putative integrase-like protein	<i>Pseudomonas</i> sp. strain KHP41	355/351	65 (209/317)	CAA67462.1	1.00E–113

<sup>a</sup> Letters indicate coding strand: c, complementary strand; d, direct strand.

<sup>b</sup> N/A, not applicable.

<sup>c</sup> Number of amino acids in pADP-1 ORF/number in the closest relative.

<sup>d</sup> Values in parentheses refer to numbers of amino acids with identity per total number examined.

nested transposon structure and contains all of the genes necessary for the degradation of atrazine to cyanuric acid, a complete mercury resistance operon, and several copies of different transposable elements.

Some of the inverted repeats postulated to be involved in the acquisition of foreign DNA in pR751 are also present in pADP-1 (59). All the inverted repeats in the area between *oriV* and *trfA* on pR751 except for inverted repeat 4, are present and highly conserved in pADP-1. In addition, the inverted repeats in pR751 between *upf54.4* (*traO*) and *traM* are present and highly conserved in pADP-1. However, the inverted repeats present in the areas between Tra1-Tn402 and Tn402-Tra2 in pR751 were not found in the pADP-1 genome.

**Transposition and integration-related ORFs.** About 15% of the identified ORFs in the pADP-1 sequence had significant identity to proteins involved in DNA integration and transposition. Three ORFs (ORF34, ORF41, and ORF49) in the pADP-1 sequence had >99% amino acid sequence identity to TnpA from IS1071. Two IS1071 insertion elements flank the

atrazine chlorohydrolase gene, *atzA* (ORF37), while the third copy is located approximately 6 kb downstream of the hydroxyatrazine ethylaminohydrolase (*atzB*) gene (ORF44). A truncated copy of transposase TnpA from IS1071 was localized at nucleotide positions 75908 to 76264 near the *trb* operon (Fig. 3). The 110-bp inverted repeats normally associated with IS1071 are present in the homologs found on pADP-1. In addition, a partial copy (69 nucleotides) of these inverted repeats was found between the *istB* and the *traC* genes. DNA fragments homologous to the *pdhL* and *pdhB* genes were found to flank most of the copies of IS1071 present on pADP-1. These genes encode different components of the pyruvate dehydrogenase enzyme complex (26). The IS1071 copies present in pADP-1 (Table 1) always interrupt *pdhL* at the same position, suggesting that *pdhL* is a target for the insertion of this transposon.

Four ORFs, ORF32 (nucleotides 27514 to 29061), ORF39 (37037 to 38584), ORF47 (48776 to 50323), and ORF73 (72897 to 74444), had >99% amino acid sequence identity to an

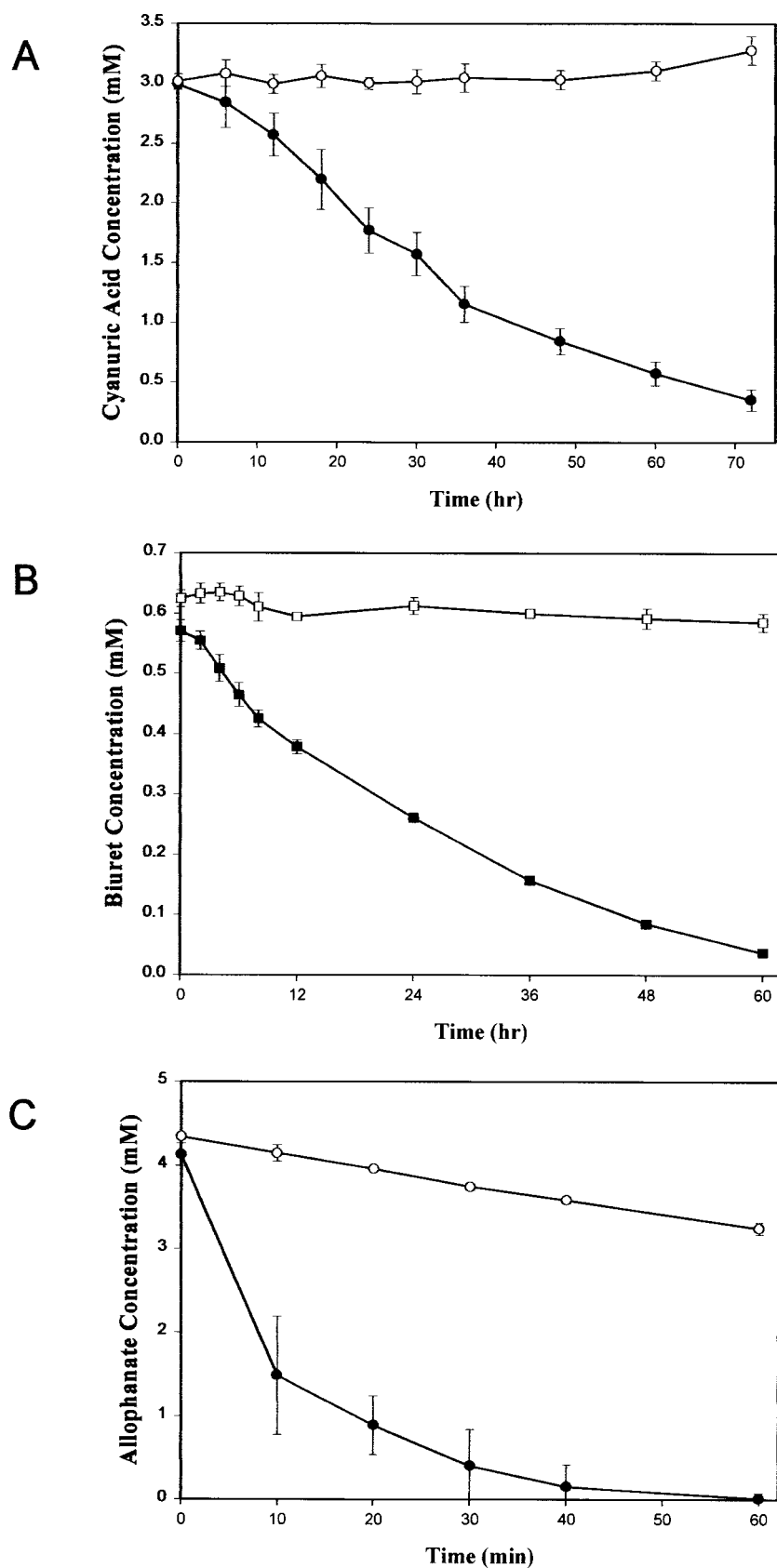


FIG. 4. (A) Degradation of cyanuric acid by crude cell extracts from *E. coli* DH5 $\alpha$ (pBMZ1). Plasmid pBMZ1 contains *atzD* from pADP-1 cloned into the *Bam*HI site of pKT230. Symbols: ●, *E. coli* DH5 $\alpha$ (pBMZ1); ○, *E. coli* DH5 $\alpha$ . (B) Degradation of biuret by crude cell extracts from *E. coli* DH5 $\alpha$  (*atxE*). Symbols: ■, *E. coli* DH5 $\alpha$  (*atxE*); □, *E. coli* DH5 $\alpha$ (pUC18). (C) Degradation of allophanate by crude cell extracts of *E. coli* DH5 $\alpha$  (*atxF*). Symbols: ●, *E. coli* DH5 $\alpha$  (*atxF*); ○, *E. coli* DH5 $\alpha$ (pUC18). Values are the means of three replicates. Bars indicate standard deviations of the mean.

IS801-like transposase (TnpA) previously identified in *Pseudomonas pseudoalcaligenes* JS45 (14). Complete copies of this transposase were identified on the opposite strand flanking the *atzA* and *atzB* genes and on the same strand upstream of the *atzC* gene (ORF71) (Fig. 3). No inverted repeat structures were found in the DNA regions surrounding these transposases. However, 187-bp and 108-bp conserved DNA regions were consistently found, upstream and downstream, respectively, of the IS801-like *tnpA* genes in pADP-1. These sequences were also found in the same positions in IS801-like genes present in *Acidovorax avenae* subsp. *citrulli* (accession number AF086815.2), *Pseudomonas huttiensis* (accession number AF028594), and *Pseudomonas pseudoalcaligenes* (14). These conserved regions have 40% identity to each other, do not contain direct or inverted repeats, and have no homology to other well-characterized transposons.

We also identified additional ORFs with homology to transposases from organisms of diverse genera. For example, ORF 68 (nucleotides 66429 to 67739) had 45% identity to a putative transposase from *Acetobacter pasteurianus* (58), ORF70 (69053 to 70021) had 66% identity to a transposase from *Ralstonia solanacearum* (Y. A. Lee, unpublished data; GenBank accession no. AAD49338), and ORF92 (90795 to 92165) was 29% identical to a putative transposase from *Streptococcus pyogenes* (6). In addition, our analysis revealed the presence of ORF104 (107219 to 108286), which had 69% sequence identity to an integrase-like protein from Tn5041 in *Pseudomonas* sp. strain KHP41 (33). Two ORFs, ORF28 (24327 to 25175) and ORF29 (25159 to 25416), had homology to the IstB and IstA proteins from *Ralstonia eutropha*, respectively (51). In plasmids carrying the insertion sequence IS21, *istAB* are usually transcribed as part of an operon (51). In pADP-1, the IstB homolog appears complete, while the IstA homolog (ORF29) is truncated.

The complete nucleotide sequence of pADP-1 revealed the presence of several genes involved in catabolism (Table 1 and Fig. 3). These genes and gene families are discussed below in detail.

**Atrazine catabolic genes.** Sequence analysis showed that three previously identified genes involved in the initial steps of atrazine catabolism, *atzA*, *atzB*, and *atzC* (9, 15, 47), are localized to different regions of pADP-1 and are not organized in an operon-like structure. The first enzyme, AtzA, catalyzes the hydrolytic dechlorination of atrazine, yielding hydroxyatrazine. The second enzyme, AtzB, catalyzes hydroxyatrazine deamidation, yielding *N*-isopropylammelide, and the third, AtzC, encodes *N*-isopropylammelide isopropylaminohydrolase activity, stoichiometrically catabolizing *N*-isopropylammelide to cyanuric acid and *N*-isopropylamine. Consistent with our previously reported cosmid sequencing efforts, the *atzA* and *atzB* genes are located about 8 kb apart on pADP-1 (9). The *atzC* gene is located about 34 and 25 kb from the *atzA* and *atzB* genes, respectively. Sequence analysis confirmed that the G+C content of *atzC* (44%) was lower than those of *atzA* (58%) and *atzB* (61%) and most of the other genes present in the pADP-1 sequence. This result suggests that *atzC* was acquired from an organism with vastly different G+C content (47).

**New catabolic genes involved in atrazine catabolism.** ORF100 (nucleotides 101053 to 102144) had 58% amino acid identity to TrzD, a cyanuric acid amidohydrolase from *Pseudomonas* sp.

strain NRRLB-12227 (30). Since AtzC in *Pseudomonas* sp. strain ADP transforms *N*-isopropylammelide to cyanuric acid, we postulated that cyanuric acid was transformed by a similar enzyme in this bacterium. However, we previously were unsuccessful in using a *trzD* gene probe to find this gene in *Pseudomonas* sp. strain ADP or to demonstrate transformation of cyanuric acid in *E. coli* AD256(pADP-1) (M. L. de Souza and I. R. Fruchey, personal communication). To determine whether ORF100 functionally encoded cyanuric acid amidohydrolase in *Pseudomonas* sp. strain ADP, PCR was used to clone a 1.4-kb DNA fragment from pADP-1 into the *Bam*HI site of pKT230, resulting in plasmid pBMZ1. Crude extracts of *E. coli* DH5 $\alpha$  and *E. coli* DH5 $\alpha$ (pBMZ1) were tested for their ability to hydrolyze cyanuric acid, as evidenced by HPLC analysis. Results in Fig. 4A show that crude extracts of *E. coli*(pBMZ1) had the ability to hydrolyze cyanuric acid, whereas the control *E. coli* strain did not transform this substrate. Mass spectrophotometric studies done using crude cell extracts of *E. coli* (pBMZ1) and cyanuric acid as the substrate indicated that biuret is the product of this reaction (I. R. Fruchey, unpublished data). These results indicate that pADP-1 encodes a functional cyanuric acid amidohydrolase that is homologous to TrzD. This enzyme, AtzD, is encoded in the region between *oriV* and *trfA*. We are currently in the process of purifying and characterizing AtzD, and these results will be presented elsewhere.

Two ORFs, ORF101 and ORF102, were located directly downstream of *atzD*. ORF101 (102427 to 103800) had 37% sequence identity with a nicotinamidase/pyrazinamidase from *Mycobacterium smegmatis* (8) (GenBank accession no. AAC 77368), while ORF102 (104283 to 106100) had 44% sequence identity to urea amidolyase from *Saccharomyces cerevisiae* (GenBank accession no. CAA85172) (24, 57, 63). Multiple sequence alignments revealed that ORF101 and ORF102 had conserved sequence signatures diagnostic of an amidase protein family (Fig. 5) (34, 43). The residues corresponding to Asp184 and Ser188 in ORF102 and Asp169 and Ser173 in ORF101 are conserved in all the members of this amidase family. In addition, the residues corresponding to Lys90, Ser164, Ser165, Ser188, and Arg190 in ORF102 and Lys73, Ser149, Ser150, Ser173, and Arg175 in ORF101 are conserved in all the members of this same amidase family (34, 43). Mutagenesis studies have shown that these five residues are critical for the amidase activity of fatty acid amide hydrolase, a mammalian amidase that hydrolyses fatty acid amides (43). Based on our observations, we propose here that ORF101 and ORF102 are new members of this amidase family.

Growth studies indicated that *Pseudomonas putida* PRS2000 (pADP-1) transconjugants had the ability to use cyanuric acid as the sole nitrogen source (data not shown), while the wild-type strain did not. This result indicated that the gene(s) necessary for further catabolism of cyanuric acid was present on pADP-1. Since biuret is the product of cyanuric acid degradation in *Pseudomonas* sp. strains ADP and NRRLB-12227 and contains multiple amide bonds, the data suggested that ORF101 and ORF102 were involved in biuret metabolism. To experimentally determine whether these ORFs encoded a functional biuret amidohydrolase, *E. coli*(p11A07) and *E. coli* (p14D12), containing ORF101 and ORF102, respectively, were spotted onto the surface of LB agar medium containing 4,000  $\mu$ g of biuret per ml. While a clear zone surrounding cell

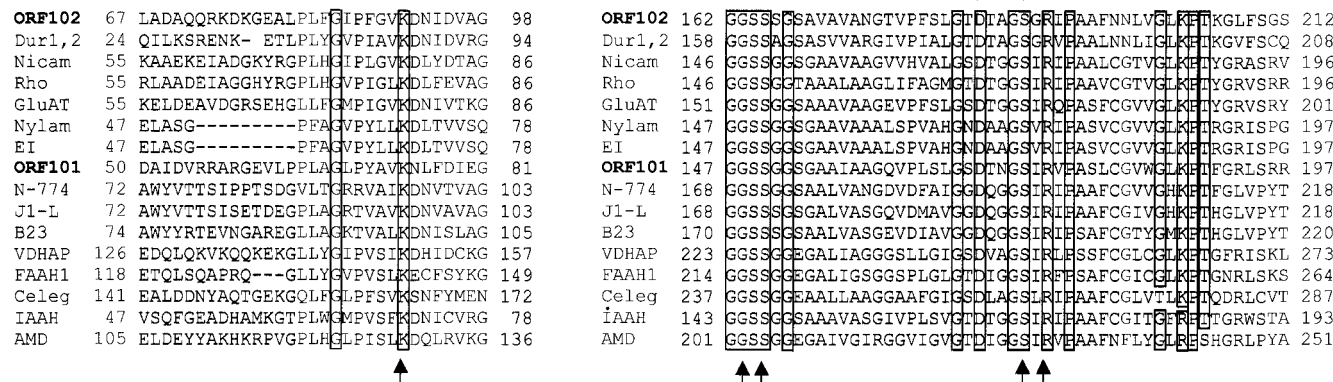


FIG. 5. Sequence alignment of ORF101 and ORF102 with members of the amidase protein family. Identical amino acids are boxed. The arrows indicate residues that have been shown to be important for amidase activity in a fatty acid amide hydrolase (FAAH). Residues common to the amidases and aspartic proteases are denoted by the asterisks. The amidase sequences used for the alignment were as follows: ORF102 from the pADP-1 plasmid sequence; Dur (1, 2), urea amidolyase from *Saccharomyces cerevisiae* (accession number CAA85172); Nicam, nicotinamidase from *Mycobacterium smegmatis* (accession number AAC77368.1); Rho, amidase from *Rhodococcus* (accession number M74531); GluAT, Glu-tRNA amidotransferase from *Bacillus subtilis* (accession number gi:25899195); Nylam, 6-aminohexanoate cyclic dimer hydrolase, *Flavobacterium* sp. (accession number gi:148711), EI, 6-aminohexanoate-cyclic-dimer hydrolase from *Flavobacterium* sp. (accession number M26953); ORF101 from the pADP-1 plasmid sequence; N-774, amidase from *Rhodococcus* sp. strain N-774 (accession number X54074); J1-L, amidase from *Rhodococcus rhodochrous* J1 (accession number D16207); B23, amidase from *Pseudomonas chlororaphis* (accession number D90216); VDHAP, vitamin D<sub>3</sub> hydroxylase-associated protein, *Gallus domesticus* (accession number gi:1079452); FAAH1, fatty acid amide hydrolase, *Rattus norvegicus* (accession number gi:1680722); Celeg, predicted amidase from *Caenorhabditis elegans* (accession number gi:6425411); IAAH, indoleacetamide hydrolase, *Pseudomonas syringae* (accession number gi:77820); AMD, acetamidase, *Emericella nidulans* (accession number gi:101782).

growth of *E. coli* DH5 $\alpha$ (p11A07) was found after 7 days of incubation, no such zone was detected with *E. coli*(p14D12) or the *E. coli*(pUC18) negative control (data not shown). To confirm these results, cell extracts from *E. coli* DH5 $\alpha$ (p11A07) were examined for biuret hydrolysis using HPLC and ammonia release assays. HPLC analyses showed that crude extracts of *E. coli* DH5 $\alpha$ (p11A07) hydrolyzed biuret, while *E. coli* DH5 $\alpha$ (pUC18) did not degrade this substrate (Fig. 4B). Ammonia release assays showed that ORF101 hydrolyzed biuret with a specific activity of approximately 3 nmol of ammonia per min per mg of protein (data not presented). The product(s) of biuret hydrolysis by ORF101 was examined by using TLC and HPLC analyses. Allophanate was detected by both methods, but only in the reaction mixtures containing biuret and crude-cell extracts from *E. coli* DH5 $\alpha$ (p11A07) (data not shown). Taken together, these results indicate that ORF101 encodes a functional biuret hydrolase that is part of the atrazine degradation pathway present in *Pseudomonas* sp. strain ADP. Based on these observations, ORF101 was designated *atzE*.

ORF102 (nucleotides 104283 to 106100), located downstream of *atzE*, was found to have 44% sequence identity to the allophanate hydrolase domain of urea amidolyase from *S. cerevisiae*. To determine if ORF102 was also involved in the atrazine degradation pathway, we examined *E. coli*(p14D12), containing a complete copy of ORF102, for its ability to hydrolyze urea or allophanate. HPLC results in Fig. 4C show that cell extracts from *E. coli*(p14D12) had allophanate hydrolase activity. In contrast, only limited loss of allophanate was seen with extracts from *E. coli*(pUC18), most likely due to the long assay time and well-known instability of allophanate in aqueous solution (63). Based on this result, ORF102 was designated *atzF*. Ammonia release assays indicated that cell extracts of *E. coli*(p14D12) failed to hydrolyze urea or biuret (Fig. 6).

The results in Fig. 6 also show that a cell extract from *E. coli*

(p11A07) (producing *AtzE*) incubated with biuret released three times more ammonia when combined with *E. coli* (p14D12) (producing *AtzF*) than in reactions containing only biuret hydrolase. Since *AtzF* does not hydrolyze biuret or urea, these results confirm that allophanate is the product of biuret hydrolysis by *AtzE*. Taken together, these results indicate that all genes necessary for the catabolism of atrazine to ammonia and carbon dioxide are localized on pADP-1 and that the last

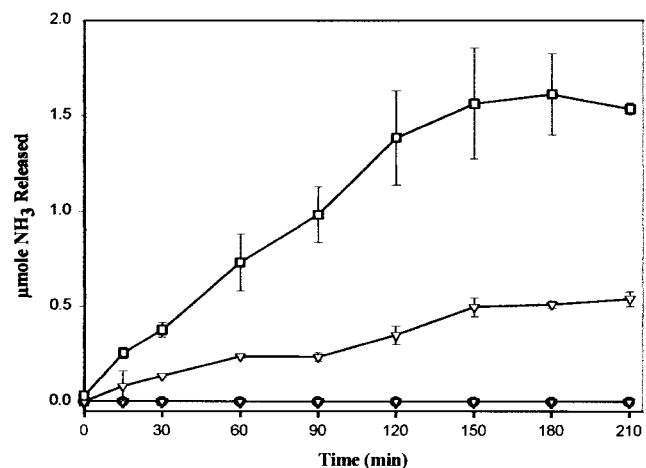


FIG. 6. Ammonia released after incubation of biuret with cell extracts from *E. coli* DH5 $\alpha$  (*atzE*) and *E. coli* DH5 $\alpha$  (*atzF*). Symbols:  $\square$ , 3 mM biuret plus crude cell extracts from *E. coli* DH5 $\alpha$  (*atzE*);  $\nabla$ , 3 mM biuret plus cell extract from *E. coli* DH5 $\alpha$  (*atzF*);  $\circ$ , 3 mM urea plus cell extract from *E. coli* DH5 $\alpha$  (*atzF*);  $\bullet$ , 3 mM biuret plus cell extract from *E. coli* DH5 $\alpha$ (pUC18). Values are the means of results from three replicates. Error bars indicate standard deviations of the means.

three genes in the atrazine degradation pathway, *atzD*, *atzE*, and *atzF*, are located in a contiguous cluster in the pADP-1 plasmid.

ORF99 (nucleotides 99885 to 100853) had 39% identity to members of the LysR family of transcriptional regulators (50). ORF99 is divergently transcribed from *atzD* and located 166 bp from the start codon of this gene. Moreover, ORF99, *atzD*, *atzE*, and *atzF* have similar mol% G+C contents (59 to 61%) and codon usage, suggesting that these four genes constitute an operon-like structure on pADP-1. To determine whether the *atzD*, *atzE*, and *atzF* genes are transcribed as a single mRNA, we used RT-PCR and primers designed to amplify contiguous cDNAs between *atzD* and *atzE* and from *atzE* to *atzF*. RT-PCR analyses showed that a single transcript of 2.3 kb was obtained using the *atzD* and *atzE* primers and a 1.1-kb transcript was obtained using the *atzE* and *atzF* primer pair (data not shown). A single mRNA from *atzD* to *atzF* would be approximately 5.2 kb and difficult to amplify. Consequently, two overlapping primer pairs were used. Since these two cDNAs were derived from a contiguous DNA region containing *atzDEF*, this result indicates that these three genes are cotranscribed as a single mRNA in *Pseudomonas* sp. strain ADP.

**Other regulatory proteins.** Several other ORFs with homology to transcriptional regulators were also identified in different regions of the pADP-1 sequence. ORF45 (nucleotides 45919 to 46494) had 30% identity to the transcriptional regulators of the Tet/Acr family (2, 42). ORF66 (65433 to 65999), which is located approximately 4.2 kb downstream of the *atzC* gene, had 67% identity to a putative transcriptional regulator from *Pseudomonas aeruginosa*. Domain analysis done using Pfam showed that this ORF was related to members of the Tet<sup>r</sup> family of transcriptional regulators (2, 42).

**Mercury resistance genes.** A DNA region with high homology to genes and an operon involved in mercury resistance was identified in the pADP-1 sequence (ORFs 50 to 57, nucleotides 55067 to 59386). This approximately 4.3-kb DNA region contains eight ORFs, each of which had >99% sequence identity to proteins from the mercury resistance operon identified in *Xanthomonas* sp. strain W17 (32) (Table 1). The functionality of the putative mercury resistance operon in pADP-1 was determined by measuring mercuric reductase activity in crude extracts of *E. coli*(pADP-1) strains and by determining growth in LB medium containing different concentrations of HgCl<sub>2</sub>. Mercuric reductase activity in *E. coli* AD256(pADP-1) and *E. coli* S17-1(pADP-1) was 301 ± 18 and 387 ± 33 nmol/min/mg of protein, respectively, while the specific activity of this enzyme was 10-fold lower in the control strains (21 ± 4 and 30 ± 2 nmol/min/mg of protein for *E. coli* S17-1 and *E. coli* AD256, respectively). In addition, results from the disk diffusion assays indicated that while *E. coli* AD256(pADP-1) and *E. coli* S17-1(pADP-1) were resistant to greater than 200 µg of HgCl<sub>2</sub> per ml (inhibition zone < 1 mm), both parental control strains were inhibited for growth by 100 µg of HgCl<sub>2</sub> per ml (inhibition zone of 2.0 mm), and at 200 µg of HgCl<sub>2</sub> per ml, inhibition zones were 4.0 and 6.0 mm for *E. coli* AD256 and *E. coli* S17-1, respectively (data not shown). Taken together, these results showed that the mercury resistance operon present in pADP-1 is functional and confers on strains the ability to detoxify mercury.

**Transporters.** A cluster of type ABC transporters was identified on pADP-1. ORF94 (nucleotides 94005 to 94928) and ORF95 (94918 to 96039) are homologous to permeases of type ABC transporters from *Pseudomonas aeruginosa* (55) (GenBank accession no. AAG03528 and AAG03527, respectively), while ORF96 (96026 to 97648) had 58% identity to the ATP-binding component of the same type ABC transporter (GenBank accession no. AE004451). In addition, two ORFs (ORF46 and ORF69) had homology to a hypothetical protein and a secondary magnesium/citrate transporter, respectively. These ORFs were classified as transporters based on results obtained from domain searches done using Pfam. ORF46 (46883 to 48223) showed a significant match to a xanthine/uracil permease family of proteins, having many residues conserved in the signature sequence of this family of proteins (1, 19). In addition, hydrophobicity plots of ORF46 predicted 12 transmembrane domains, a characteristic that is commonly observed in the xanthine/uracil permease family of proteins (1, 19). Similarly, hydrophobicity plots of ORF69 (67797 to 68942) showed 12 membrane-spanning domains, and BLAST and Pfam searches showed predicted homology to a variety of transporters.

**Hypothetical proteins.** Approximately 8% of the predicted ORFs on pADP-1 sequence had homology to conserved hypothetical proteins identified in other genomes, especially to hypothetical proteins from *Pseudomonas aeruginosa*. In an attempt to identify the potential function of these predicted ORFs, sequences were analyzed to identify motifs and conserved sequence domains. ORF58 (nucleotides 59783 to 60556), ORF59 (60661 to 61119), ORF61 (62296 to 62769), ORF63 (63790 to 64593), ORF97 (97655 to 98737), and ORF98 (98776 to 99714) had no significant matches to proteins present in the Prosite, Pfam, PRINTS, and BLOCKS databases. Therefore, the function of these proteins remains unknown. However, ORF62 (62824 to 63771) and ORF30 (25315 to 26307) had a low percentage of identity to many membrane-bound proteins and transporters. The hydrophobicity plots of these ORFs predicted 6 to 10 transmembrane domains and suggested that these ORFs may be membrane-bound proteins or transport proteins. About 2% of the ORFs had no significant homology to any known proteins in the databases.

## DISCUSSION

In this study we describe the complete nucleotide sequence of catabolic plasmid pADP-1 from a *Pseudomonas* sp. strain ADP. One of the most remarkable features of plasmid pADP-1 is its high degree of relatedness to the 53.3-kb broad-host-range IncPβ plasmid pR751, initially isolated from *Enterobacter aerogenes* (59). Nearly one-half of pADP-1 consists of the pR751 backbone (Fig. 2). Members of the IncP plasmid group have been shown to be highly conserved despite the fact that they have been isolated from diverse genera of bacteria in different parts of the world (11, 54, 60). Antibiotic resistance, mercury resistance, and other catabolic genes have previously been identified on diverse IncP plasmids (11, 54). Burlage et al. (11) reported that a 30-kb DNA fragment from pR751 was conserved in the catabolic plasmids pJP4, pSS50, and pSS60. Moreover, antibiotic resistance plasmids pR906 and pR772

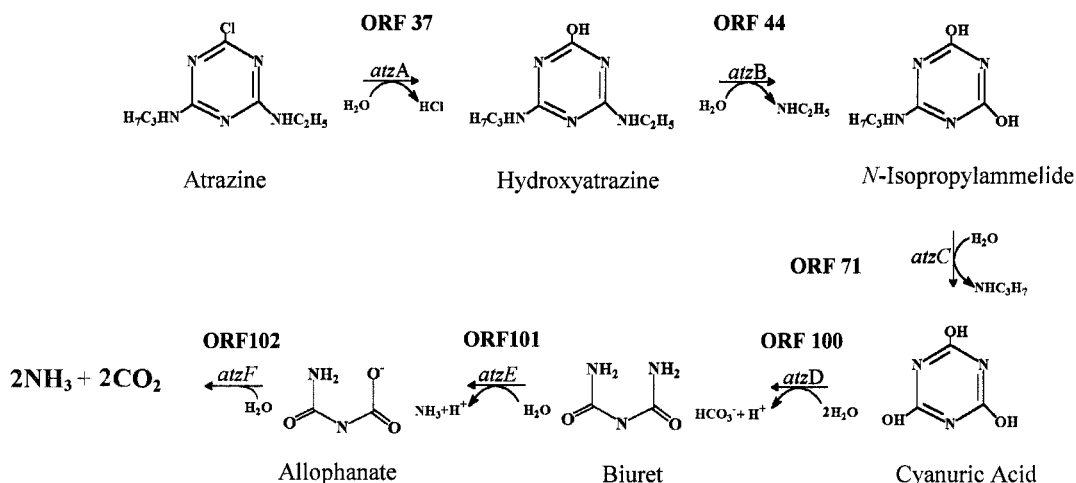


FIG. 7. Complete catabolic pathway for atrazine degradation by *Pseudomonas* sp. strain ADP. Genes and potential ORFs involved at each catabolic step are indicated.

have several loci identical to those found in pR751 (54). Similarly, Tralau and coworkers (60) mapped pTSA from *Comamonas testosteroni* T2, encoding *p*-toluenesulfonate degradation, and reported that the 72.4-kb catabolic plasmid also had a similar backbone structure.

The region of pADP-1 between the *tra* and *trb* operons (nucleotide positions 24062 to 76280) contains the *atzA*, *atzB*, and *atzC* genes. Since transposases and gene cassettes that resemble nested catabolic transposons flank *atzA*, *atzB*, and *atzC*, the atrazine catabolic genes may have been recruited at different times through independent transposition or homologous recombination events. Previously, transposase proteins from IS1071 were shown to participate in DNA insertion and recombination events in the chlorobenzoate catabolic plasmid pBR60 (39), and the operon for *p*-toluenesulfonate catabolism in *Comamonas testosteroni* has been shown to be part of a composite transposon flanked by two IS1071 elements (60).

While our previous data suggested that the gene for cyanuric acid degradation was not located on pADP-1 (17), in the present study we show, by sequence and functional analysis, that *atzD* (ORF100) hydrolyzes cyanuric acid to biuret (Fig. 4A and 7). AtzD has 58% sequence identity to TrzD from *Pseudomonas* sp. strain NRRLB-12227 (30). TrzD, which is functional in the melamine catabolic pathway, also hydrolyzes cyanuric acid (21, 22). Recently, *trzD* was localized to a self-transmissible IncIα plasmid, pPDL12, in *Klebsiella pneumoniae* (31).

Results from our cloning and functional studies show that two amidases, AtzE (ORF101) and AtzF (ORF102), are involved in the further catabolism of biuret to  $\text{CO}_2$  and  $\text{NH}_3$  (Fig. 7). These proteins are members of the same amidase family. AtzE (nucleotides 102427 to 103800) had 37% sequence identity to a nicotinamidase/pyrazinamidase from *Mycobacterium smegmatis* and was shown by three independent methods to encode a biuret hydrolase, resulting in the formation of allophanate. Previously, biuret hydrolases have been reported in cyanuric acid-degrading bacteria (13, 21, 22).

The functional studies reported here indicate that AtzF hydrolyzes allophanate to  $\text{NH}_3$  and  $\text{CO}_2$ . AtzF (nucleotides 104283 to 106100) had 44% sequence identity to the allo-

phanate hydrolase domain of urea amidolyase from *S. cerevisiae* (24, 57, 63). This domain has been shown to catalyze the hydrolysis of allophanate to 2 mol each of ammonia and carbon dioxide (63). While genome sequencing efforts have identified homologs to the *S. cerevisiae* allophanate hydrolase gene in *Bacillus subtilis* and *Campylobacter jejuni* (GenBank accession no. AL139078 and Z99106, respectively), the amino acid identity of these proteins to AtzF was low (20 and 25%, respectively). To our knowledge, this is the first report of the functional characterization of an allophanate hydrolase from a bacterium.

Previously, Cook et al. (13) reported that urea was the product of biuret degradation in *Pseudomonas* sp. strain NRRLB-12228 (strain D) and that *Klebsiella pneumoniae* strain 99 had negligible allophanate amidohydrolase activity. Likewise, Eaton and Karns (21, 22) reported that cyanuric acid was hydrolyzed to biuret and urea in *Pseudomonas* sp. strain NRRLB-12227. However, these metabolites were identified by using HPLC analyses at pH 2.0, precluding detection of the acid-labile allophanate which decomposes to urea.

The *atzD* (ORF100), *atzE* (ORF101), and *atzF* (ORF102) genes form a gene cluster, 166 bp from the divergently transcribed ORF99. RT-PCR analyses indicated that *atzDEF* are cotranscribed on a single mRNA. This physical relationship suggests that ORF99 may regulate *atzDEF*. ORF99 is predicted to encode a LysR-type transcriptional regulator and contains a DNA-binding helix-turn-helix motif at its N-terminal domain (amino acids 26 to 168). Moreover, the intergenic region between ORF99 and *atzD* (166 bp upstream of *atzD*) contains a T-N<sub>11</sub>-A DNA motif (at positions 100875 to 100887) as part of an interrupted dyad sequence. This motif has been found upstream of most LysR-type-regulated genes (50), suggesting that ORF99 may regulate the *atzDEF* genes. The exact regulatory function of ORF99 awaits further study.

While our data indicate that *atzDEF* are organized in an operon-like structure, the *atzA*, *atzB*, and *atzC* genes are dispersed on plasmid pADP-1 and flanked by many transposable elements (Fig. 2 and 3). Moreover, there is no sequence evidence for regulatory elements upstream of the *atzA*, *atzB*, or

*atzC* genes, and previous Northern hybridization studies have shown that in *Pseudomonas* sp. strain ADP, the *atzA* and *atzB* genes are transcribed in the absence of atrazine or hydroxyatrazine as inducers, respectively (M. L. de Souza, unpublished data). Taken together, these observations are consistent with the idea that the constitutively expressed *atzA*, *atzB*, and *atzC* genes were recently acquired by *Pseudomonas* sp. strain ADP and other soil bacteria. We previously reported that pADP-1 is self-transmissible to gram-negative bacteria (17) and that several genera of bacteria isolated from different geographical regions contain nearly identical atrazine catabolism genes (16). While direct plasmid transfer may appear to be a plausible mechanism for the dissemination of atrazine genes among these bacteria, we have reported that the *atzA*, *atzB*, and *atzC* genes are localized to different-sized plasmids in phylogenetically diverse microorganisms (B. Martinez, M. de Souza, L. Wackett, and M. Sadowsky, Abstr. 99th Gen. Meet. Am. Soc. Microbiol., abstr. Q352, 1999). Moreover, variants of *Pseudomonas* sp. strain ADP have been identified that contain the *atzB* and *atzC* but not the *atzA* gene (M. L. de Souza, unpublished data), some wild-type bacteria contain only the *atzA* gene (10), and individual bacteria in an atrazine-metabolizing consortium each contain an incomplete set of atrazine catabolism genes (18). Taken together, these data suggest that the atrazine catabolic genes can be recruited or lost independently and that direct plasmid transfer may not be the only mechanism by which atrazine degradation genes are disseminated in the environment.

In summary, the plasmid sequencing studies reported here revealed that all the genes for the complete metabolism of atrazine are localized on pADP-1 in *Pseudomonas* sp. strain ADP. Moreover, we show that atrazine catabolism in *Pseudomonas* sp. strain ADP occurs via a novel pathway involving an allophanate intermediate. These findings provide a window onto the apparent recent evolution of catabolic pathways in nutritionally diverse soil bacteria.

#### ACKNOWLEDGMENTS

This work was supported, in part, by grant 98-35107-6368 from the U.S. Department of Agriculture-NRI/CGP/CSREES, by a grant from Syngenta Crop Protection, Greensboro, N.C., and by the University of Minnesota Agricultural Experiment Station.

We thank Janis McFarland from Syngenta Crop Protection for providing substrates and Becky Paraless for providing *Pseudomonas putida* PRS2000(pADP-1). We also thank Isaac Fruchey for help with *atzD* and Sung-Sick Woo and Yeisoo Yu for help with sequencing and the sequence assembly software. We also thank Claire Fant and Megan Bruce-Carver for technical assistance in the sequencing laboratory, Lynda Ellis for assistance with open reading frame analyses, Gil Johnson and Jack Richman for the synthesis and NMR analysis of allophanate, and Charlotte Rosendahl for helpful discussions.

#### REFERENCES

- Andersen, P. S., D. Frees, R. Fast, and B. Mygind. 1995. Uracil uptake in *Escherichia coli* K-12: isolation of *uraA* mutants and cloning of the gene. *J. Bacteriol.* **177**:2008–2013.
- Aramaki, H., N. Yagi, and M. Suzuki. 1995. Residues important for the function of a multihelical DNA binding domain in the new transcription factor family of Cam and Tet repressors. *Protein Eng.* **8**:1259–1266.
- Austen, R. A., and N. W. Dunn. 1977. Isolation of mutants with altered metabolic control of the NAH plasmid-encoded catechol meta-cleavage pathway. *Aust. J. Biol. Sci.* **30**:583–592.
- Bagdasarian, M., R. Lurz, B. Ruckert, F. C. Franklin, M. M. Bagdasarian, J. Frey, and K. N. Timmis. 1981. Specific-purpose plasmid cloning vectors. II. Broad host range, high copy number, RSF1010-derived vectors, and a host-vector system for gene cloning in *Pseudomonas*. *Gene* **16**:237–247.
- Berg, T., N. Firth, S. Apisiridej, A. Hettiaratchi, A. Leelaporn, and R. A. Skurray. 1998. Complete nucleotide sequence of pSK41: evolution of staphylococcal conjugative multiresistance plasmids. *J. Bacteriol.* **180**:4350–4359.
- Berge, A., M. Rasmussen, and L. Bjorck. 1998. Identification of an insertion sequence located in a region encoding virulence factors of *Streptococcus pyogenes*. *Infect. Immun.* **66**:3449–3453.
- Borodovsky, M., and J. McIninch. 1993. GeneMark: parallel gene recognition for both DNA strands. *Comput. Chem.* **17**:123–133.
- Boshoff, H. I. M., and V. Mizrahi. 1998. Purification, gene cloning, targeted knockout, overexpression, and biochemical characterization of the major pyrazinamidase from *Mycobacterium smegmatis*. *J. Bacteriol.* **180**:5809–5814.
- Boundy-Mills, K. L., M. L. de Souza, R. T. Mandelbaum, L. P. Wackett, and M. J. Sadowsky. 1997. The *atzB* gene of *Pseudomonas* sp. strain ADP encodes the second enzyme of a novel atrazine degradation pathway. *Appl. Environ. Microbiol.* **63**:916–923.
- Bouquard, C., J. Quazzani, J. C. Prome, Y. M. Briand, and P. Plesiat. 1997. Dechlorination of atrazine by a *Rhizobium* isolate. *Appl. Environ. Microbiol.* **63**:862–866.
- Burlage, R. S., L. A. Bemis, A. C. Layton, G. S. Saylor, and F. Larimer. 1990. Comparative genetic organization of incompatibility group P degradative plasmids. *J. Bacteriol.* **172**:6818–6825.
- Chaudhry, G. R., and G. H. Huang. 1988. Isolation and characterization of a new plasmid from a *Flavobacterium* sp. which carries the genes for degradation of 2,4-dichlorophenoxy-acetate. *J. Bacteriol.* **170**:3897–3902.
- Cook, A. M., P. Beilstein, H. Grossenbacher, and R. Hutter. 1985. Ring cleavage and degradative pathway of cyanuric acid in bacteria. *Biochem. J.* **231**:25–30.
- Davis, J. K., G. C. Paoli, Z. He, L. J. Nadeau, C. C. Somerville, and J. C. Spain. 2000. Sequence analysis and initial characterization of two isozymes of hydroxylaminobenzene mutase from *Pseudomonas pseudoalcaligenes* JS45. *Appl. Environ. Microbiol.* **66**:2965–2971.
- de Souza, M. L., L. P. Wackett, K. L. Boundy-Mills, R. T. Mandelbaum, and M. J. Sadowsky. 1995. Cloning, characterization, and expression of a gene region from *Pseudomonas* sp. strain ADP involved in the dechlorination of atrazine. *Appl. Environ. Microbiol.* **61**:3373–3378.
- de Souza, M. L., M. J. Sadowsky, J. Seffernick, B. Martinez, and L. P. Wackett. 1998. The atrazine catabolism genes are widespread and highly conserved. *J. Bacteriol.* **180**:1951–1954.
- de Souza, M. L., L. P. Wackett, and M. J. Sadowsky. 1998. The *atzABC* genes encoding atrazine catabolism are located on a self-transmissible plasmid in *Pseudomonas* sp. strain ADP. *Appl. Environ. Microbiol.* **64**:2323–2326.
- de Souza, M. L., D. Newcombe, S. Alvey, D. E. Crowley, A. Hay, M. J. Sadowsky, and L. P. Wackett. 1998. Molecular basis of a bacterial consortium: interspecies catabolism of atrazine. *Appl. Environ. Microbiol.* **64**:178–184.
- Diallinas, G., L. Gorfinkiel, H. N. Arst, G. Cecchetto, and C. Scazzocchio. 1995. Genetic and molecular characterization of a gene encoding a wide specificity purine permease of *Aspergillus nidulans* reveals a novel family of transporters conserved in prokaryotes and eukaryotes. *J. Biol. Chem.* **270**:8610–8622.
- Dougherty, B. A., C. Hill, J. F. Weidman, D. R. Richardson, J. C. Venter, and R. P. Ross. 1998. Sequence and analysis of the 60 kb conjugative, bacteriocin-producing plasmid pMRC01 from *Lactococcus lactis* DPC3147. *Mol. Microbiol.* **29**:1029–1038.
- Eaton, R. W., and J. S. Karns. 1991. Cloning and analysis of *s*-triazine catabolic genes from *Pseudomonas* sp. strain NRRLB-12227. *J. Bacteriol.* **173**:1215–1222.
- Eaton, R. W., and J. S. Karns. 1991. Cloning and comparison of the DNA encoding ammelide aminohydrolase and cyanuric acid amidohydrolase from three *s*-triazine-degrading bacterial strains. *J. Bacteriol.* **173**:1363–1366.
- Fox, B., and C. T. Walsh. 1982. Mercury reductase: purification and characterization of a transposon-encoded flavoprotein containing an oxidation-reduction-active disulfide. *J. Biol. Chem.* **257**:2498–2503.
- Genbauffe, F. S., and T. G. Cooper. 1991. The urea amidolyase (DUR1,2) of *Saccharomyces cerevisiae*. *DNA Sequence* **2**:19–32.
- Gordon, D., C. Abajian, and P. Green. 1998. *Consed*: a graphical tool for sequence finishing. *Genome Res.* **8**:195–202.
- Hein, S., and A. Steinbuchel. 1994. Biochemical and molecular characterization of the *Alcaligenes eutrophus* pyruvate dehydrogenase complex and identification of a new type of dihydrolipoamide dehydrogenase. *J. Bacteriol.* **176**:4394–4408.
- Hirsch, P. R., M. van Montagu, A. W. B. Johnston, N. J. Brewin, and J. Schell. 1980. Physical identification of bacteriocinogenic, nodulation, and other plasmids in strains of *Rhizobium leguminosarum*. *J. Gen. Microbiol.* **120**:403–412.
- Holben, W. E., and D. Harris. 1995. DNA-based monitoring of total bacteria community structure in environmental samples. *Mol. Ecol.* **4**:627–631.
- Hu, P., J. Elliot, P. McCreedy, E. Skowronski, J. Garnes, A. Kobayashi, R. R. Brunaker, and E. Garcia. 1998. Structural organization of virulence-associ-

- ated plasmids of *Yersinia pestis*. J. Bacteriol. **180**:5192–5202.
30. Karns, J. 1999. Gene sequence and properties of a *s*-triazine ring-cleavage enzyme from *Pseudomonas* sp. strain NRRLB-12227. Appl. Environ. Microbiol. **65**:3512–3517.
  31. Karns, J. S., and R. W. Eaton. 1997. Genes encoding *s*-triazine degradation are plasmid-borne in *Klebsiella pneumoniae* strain 99. J. Agric. Food Chem. **45**:1017–1022.
  32. Kholodii, G. Y., O. V. Yurieva, O. L. Lomovskaya, Z. H. M. Gorlenko, S. Z. Mindlin, and V. G. Nikiforov. 1993. Tn5053, a mercury resistance transposon with integron's ends. J. Mol. Biol. **230**:1103–1107.
  33. Kholodii, G. Y., S. Z. Mindilin, Z. M. Gorlenko, I. A. Bass, E. S. Kalyaeva, and V. Nikiforov. 2000. Molecular genetic analysis of the Tn5041 transposition system. Russ. J. Genet. **36**:365–373.
  34. Kobayashi, M., Y. Fujiwara, M. Goda, H. Kameda, and S. Shimizu. 1997. Identification of active sites in amidase: evolutionary relationship between amide bond- and peptide bond-cleaving enzymes. Proc. Natl. Acad. Sci. USA **94**:11986–11991.
  35. Kobel, M., and M. Elsener. 1995. Determination of urea and its thermal decomposition products by high performance liquid chromatography. J. Chromatogr. A **689**:164–169.
  36. Lederberg, J. 1952. Cell genetics and hereditary symbiosis. Physiol. Rev. **32**:403–430.
  37. Lukashin, A. V., and M. Borodovsky. 1998. GeneMark.hmm: new solutions for gene finding. Nucleic Acids Res. **26**:1107–1115.
  38. Mandelbaum, R. T., D. L. Allan, and L. P. Wackett. 1995. Isolation and characterization of a *Pseudomonas* sp. that mineralizes the *s*-triazine herbicide atrazine. Appl. Environ. Microbiol. **61**:1451–1457.
  39. Nakatsu, C., J. Ng, R. Singh, N. Strais, and C. Wyndham. 1991. Chlorobenzoate catabolic transposon Tn5271 is a composite class I element with flanking class II insertion sequences. Proc. Natl. Acad. Sci. USA **88**:8316–8321.
  40. Nusslein, K., and J. M. Tiedje. 1998. Characterization of the dominant and rare members of a young Hawaiian soil bacterial community with small-subunit ribosomal DNA amplified from DNA fractionated on the basis of its guanine and cytosine composition. Appl. Environ. Microbiol. **64**:1283–1289.
  41. Okinaka, R. T., K. Cloud, O. Hampton, A. R. Hoffmaster, K. K. Hill, P. Keim, T. M. Koehler, G. Lamke, S. Kumano, J. Mahillon, D. Manter, Y. Martinez, D. Ricke, R. Svensson, and P. J. Jackson. 1999. Sequence and organization of pX01: the large *Bacillus anthracis* plasmid harboring the anthrax toxin genes. J. Bacteriol. **181**:6509–6515.
  42. Pabo, C. O., and R. T. Sauer. 1992. Transcriptional factors: structural families and principles of DNA recognition. Annu. Rev. Biochem. **61**:1053–1095.
  43. Patricelli, M. P., and B. F. Cravatt. 2000. Clarifying the catalytic roles of conserved residues in the amidase signature family. J. Biol. Chem. **275**:19177–19184.
  44. Radosevich, M., S. M. Traina, Y. L. Hao, and O. H. Tuovinen. 1995. Degradation and mineralization of atrazine by a soil bacteria isolate. Appl. Environ. Microbiol. **61**:297–302.
  45. Rheinwald, J. G., A. M. Chakrabarty, and I. C. Gunsalus. 1973. A transmissible plasmid controlling camphor oxidation in *Pseudomonas putida*. Proc. Natl. Acad. Sci. USA **70**:885–889.
  46. Romine, M. F., L. C. Stillwell, K. K. Wong, S. J. Thurston, E. C. Sisk, C. Sensen, T. Gaasterland, J. K. Fredrickson, and J. D. Saffer. 1999. Complete sequence of 184-kilobase catabolic plasmid from *Sphingomonas aromatica* F199. J. Bacteriol. **181**:1585–1602.
  47. Sadowsky, M. J., Z. Tong, M. de Souza, and L. P. Wackett. 1998. AtzC is a new member of the amidohydrolase protein superfamily and is homologous to other atrazine-metabolizing enzymes. J. Bacteriol. **180**:152–158.
  48. Sambrook, J., E. F. Fritsch, and T. Maniatis. 1989. Molecular cloning: a laboratory manual, 2nd ed. Cold Spring Harbor Laboratory Press, Cold Spring Harbor, N.Y.
  49. Saylor, G. S., S. W. Hooper, A. C. Layton, and J. M. King. 1990. Catabolic plasmids of environmental and ecological significance. Microb. Ecol. **19**:1–20.
  50. Schell, M. A. 1993. Molecular biology of the LysR family of transcriptional regulators. Annu. Rev. Microbiol. **47**:597–626.
  51. Schmid, S., T. Seitz, and D. Hass. 1998. Cointegrase, a naturally occurring, truncated form of IS21 transposase, catalyzes replicon fusion rather than simple insertion of IS21. J. Mol. Biol. **282**:571–583.
  52. Sherburn, C. K., T. D. Lawley, M. W. Gilmour, F. R. Blattner, V. Burland, E. Grotbeck, D. J. Rose, and D. Taylor. 2000. The complete nucleotide sequence and analysis of R27, a large IncHI plasmid from *Salmonella typhi* that is temperature sensitive for transfer. Nucleic Acids Res. **28**:2177–2186.
  53. Simon, R., U. Priefer, and A. Puhler. 1983. A broad host range mobilization system for *in vivo* genetic engineering: transposon mutagenesis in gram negative bacteria. Bio/Technology **1**:784–791.
  54. Smith, C. M., and C. M. Thomas. 1987. Comparison of the organization of the genomes of phenotypically diverse plasmids of incompatibility group P: members of the IncPβ subgroup are closely related. Mol. Gen. Genet. **206**:419–427.
  55. Stover, C. K., X. Q. Pham, A. L. Erwin, S. D. Mizoguchi, P. Warrenner, M. J. Hickey, F. S. Brinkman, W. O. Hufnagle, D. J. Kowalik, M. Lagrou, R. L. Garber, L. Goltry, E. Tolentino, S. Westbrock-Wadman, Y. Yuan, L. L. Brody, S. N. Coulter, K. R. Folger, A. Kas, K. Larbig, R. Lim, K. Smith, D. Spencer, G. K. Wong, Z. Wu, and I. T. Paulsen. 2000. Complete genome sequence of *Pseudomonas aeruginosa* PAO1: an opportunistic pathogen. Nature **406**:959–964.
  56. Summers, W. 1970. A simple method for extraction of RNA from *E. coli* utilizing diethylprocarbonate. Anal. Biochem. **33**:459–463.
  57. Sumrada, R. A., and T. G. Cooper. 1982. Urea carboxylase and allophanate hydrolase are components of multifunctional protein in yeast. J. Biol. Chem. **257**:9119–9127.
  58. Takemura, H., S. Horinouchi, and T. Beppu. 1991. Novel insertion sequence IS1380 from *Acetobacter pasteurianus* is involved in the loss of ethanol-oxidizing ability. J. Bacteriol. **173**:7070–7076.
  59. Thorsted, P. B., D. P. Marcanteny, P. Akhtar, A. S. Haines, N. Ali, P. Davidson, T. Stafford, M. J. Pocklington, W. Pansegrau, B. M. Wilkings, E. Lanka, and C. Thomas. 1998. Complete sequence of the IncPβ plasmid R751: implications for the evolution and organisation of the IncP backbone. J. Mol. Biol. **282**:969–990.
  60. Tralau, T., A. M. Cook, and J. Ruff. 2001. Map of the IncP1β plasmid pTSA encoding the widespread genes (*isa*) for p-toluenesulfonate degradation in *Comamonas testosteroni* T2. Appl. Environ. Microbiol. **67**:1508–1516.
  61. Weatherburn, M. W. 1967. Phenol-hypochlorite reaction for the determination of ammonia. Anal. Chem. **39**:971–974.
  62. Weiss, A. A., S. D. Murphy, and S. Silver. 1977. Mercury and organomercurial resistances determined by plasmids in *Staphylococcus aureus*. J. Bacteriol. **122**:197–208.
  63. Whitney, P. A., and T. G. Cooper. 1972. Urea carboxylase and allophanate hydrolase. Two components of adenosine triphosphate:urea amidolyase in *Saccharomyces cerevisiae*. J. Biol. Chem. **247**:1349–1353.
  64. Williams, P. A., and K. Murray. 1974. Metabolism of benzoate and the methylbenzoates by *Pseudomonas putida* (arvilla) mt-2: evidence for the existence of a TOL plasmid. J. Bacteriol. **1**:416–423.